Two Experiments Involving the Detection of 14 MeV Neutrons.

by

R. Malcolm

Submitted in partial fulfillment
of the requirements for the degree of
Master of Science.

Department of Physics,
Faculty of Pure and Applied Science,
The University of Ottawa,
Ottawa, Canada.

1965

Approved for the Department of Physics

Supervisor

Chairman of the
Examining Committee

Chairman of the
Department

To Claire.

Without whose patience and persistence much of this would still be undone.

ABSTRACT

PART I

An existing Time-of-Flight system was improved so that 14 MeV neutrons, after striking an oxygen target, could be detected with sufficient resolution to indicate whether the state excited was at 6 or 7 MeV.

The new data obtained concerning angular distributions was compared with previous data, and agreement was sought with several theoretical models.

PART II

Several detection devices, suitable for a spectrometer, which could operate with neutrons up to 14 MeV of energy were tried. One of the devices, a $Li^6I(Eu)$ crystal, cooled to the temperature of liquid air, proved quite promising. Once the difficulties of obtaining a good crystal are overcome, it appears that this device is quite suitable for studying neutron induced reactions in shielding materials.

ACKNOWLEDGEMENTS

The author would like to express his thanks to:

Prof. Robson for suggesting the problems undertaken, and providing assistance, both technical and administrative;

Dr. W. J. MacDonald for the opportunity to partake in his experiment, use his equipment, and for the many hours of patient explanation demanded of him;

The professors and graduate students of the physics department for the many ideas and helpful inovations they provided;

The technicians of the department who built and maintained most of the equipment, and helped in their design.

TABLE OF CONTENTS

LIST OF DIAGRAMS

PREFACE

The work done for this thesis was in two parts. The first problem attempted was that of finding a suitable apparatus or detector to do experiments on shielding material. However, the time required to manufacture one of the devices tested was about 3 months, and it was felt that this time could be well used by participating in another experiment.

Dr. W. J. MacDonald proposed an experiment which involved improving a system he had built previously, and using it to make further measurements on inelastic scattering of neutrons from O^{16}. When this work was completed, the $Li^{6}I(Eu)$ crystal ordered in conjunction with the first experiment had arrived, and a continuation of the original work was undertaken.

The apparatus of Dr. MacDonald was used in one part of the work on detectors for the shielding experiment, and so the part of the thesis which concerns this apparatus is presented first, in order that the reader will have some familiarity with it when it is discussed in conjunction with detectors.

PART I

INTRODUCTION

In the Independent particle model of the nucleus, one can think of the excitations of the nucleus as belonging to two classes; those arising from collective motions of a relatively inert core, and excitations of nucleons and/or rotation of a more loosely bound cloud. The nucleus of O^{16} can be thought of as only a core, with no cloud around it. An understanding of the excitations of this nucleus is essential in explaining the excitation of heavier nucleii which have both cloud and core nucleons.

The so called "Giant Resonance" which occurs in all nucleii can be explained as a dipole motion of the protons againt the neutrons, with an excitation energy of about 20 MeV. Many examples of a collective octupole motion of the core at a few MeV are also known and quadrupole motions with excitation energy of about 12 MeV have also been observed[3].

The explanation of these motions assume that the nuclear forces are strong enough that the nucleus can be described as a liquid drop. There is question as to whether a nucleus as light as O^{16} can be accurately described in terms of a drop of liquid.

There is a -6.13 MeV 3^- state in O^{16} which might be a collective octupole motion, and which was the object of some of the work described in a thesis by W. J. MacDonald[1]. However the data obtained in that experiment was not accurate enough to give

conclusive results, and the present work was undertaken to improve the data. In particular, there is a -7 MeV state which could not be clearly distinguished from the -6 MeV state which was of interest.

The original work attempted to fit the data to theoretical predictions based on the Distorted Wave Born Approximation model (App. B), assuming an octupole deformation, but the agreement was poor.

Several explanations were offered. Over-estimation of the -7 MeV peak could give rise to the results obtained. An improvement in the apparatus used could overcome this, and if the data still did not fit the predictions, one could conclude that either a light nucleus could not be thought of as an incompressible fluid, or that the optical model itself was a poor assumption. The latter may arise because the surface of a light nucleus may be too irregular to be described in terms of a smooth optical potential.

Neutrons of 14.1 MeV were obtained for the experiment from a 100 KeV charged particle accelerator using the $T(D, n)\alpha$ reaction. The Tritium was absorbed in a zirconium plated copper disc, and the Deuterons were allowed to impinge on the plate which was held at the end of the accelerator. The resulting neutrons and alpha particles are emitted in opposite directions, because of conservation of momentum, and since both are created at the same time, one can tell when the neutron was created, and in what direction it is travelling by observing the associated alpha particle. These neutrons are allowed to scatter from the target of interest, which is set a known distance from the source, see Fig. 1. The scattered neutrons then traverse a known distance before being detected. If the transit time is measured, then the energy of the scattered neutron can be calculated, and from this one can infer the excitation energy

Fig. 1

Neutron time of flight apparatus (not to scale).

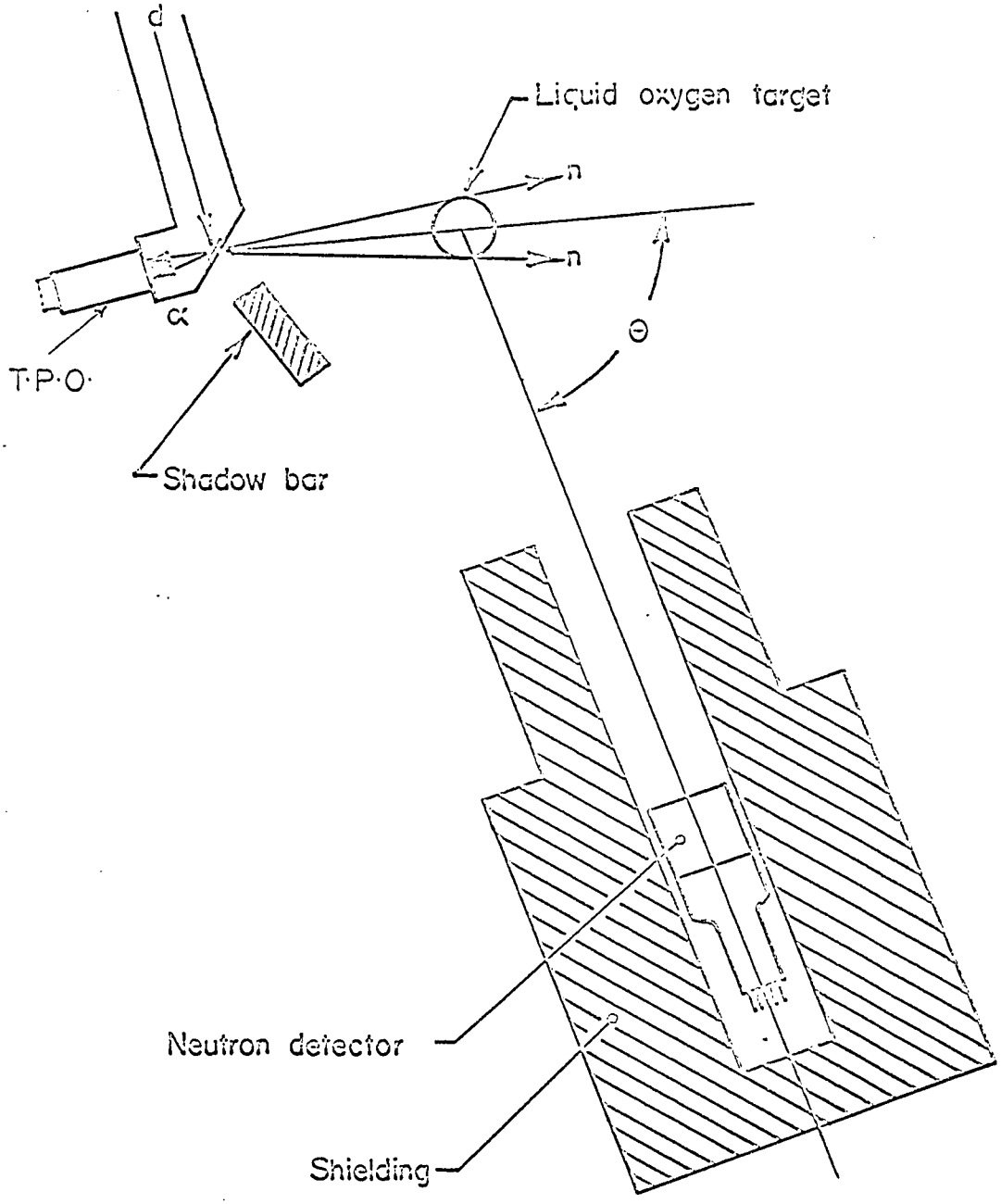

Neutron time of flight apparatus (not to scale).

of the target nucleus. By counting the number of alpha particles as well as the number of coincidences, one may measure the differential scattering cross-section. Repeating the experiment at several angles then yields the angular distribution.

The original apparatus had a resolution, expressed as the full width at half maximum of the peak corresponding to the flight time of neutrons of a particular energy, which was 2.5 n sec. A 7 MeV neutron has a velocity of 3.54×10^{-2} m/n sec., while that of an 8 MeV neutron is 3.84×10^{-2} m/n sec. Thus a 7 MeV neutron will traverse 1 metre in 28.3 n sec. while the 8 MeV neutron will take 26.1 n sec. The time difference between these is 2.2 n sec. Let R be the time resolution of the time of flight system. In order to resolve peaks arising from neutrons traversing this distance, there should be a time corresponding to 3/2 R between their centres. i.e. 3/2 R = 2.2 n sec or R should be 1.5 n sec. per metre if 7 MeV neutrons are to be distinguished from those having 8 MeV of energy over a path difference of one metre.

Experiment.

The scintillation device used for the detection of the associated alpha particles in the original apparatus gave out pulses of varying height which were then used to saturate a pre-amplifier. The time required to reach saturation varied with the height of the input pulse, and this caused uncertainty in the time of arrival of the alpha particle, which resulted in an error in the flight time of the neutron.

A junction detector gives off uniform pulses for these alpha particles and a "surface barrier" type was selected for this experiment. However, these devices give only a very small output pulse, and so some means of amplifications was necessary.

A time-pick-off unit (ORTEC Model 260) is designed to obtain a timing signal directly from a semi-conductor detector without significantly altering the energy resolution of the detector - linear amplifier system. It consists of a pulse transformer, a wide-band transistor amplifier, a tunnel diode discriminator, and a line-driver buffer. The pulse current from the detector flows through the primary of the pulse transformer en route to the pre-amplifier. (See Fig. 2). The output from this unit is a .5 volt negative pulse which corresponds to the leading edge of any input signal which exceeds a variable bias on the tunnel diode.

The linear pre-amplifier output was fed through a single channel analyser which was used to select only those pulses which corresponded to the desired alpha particles.

The time-pick-off unit "sees" dq/dt. where q is charge and t is time, and this rate is a function of the input capacity and resistance of the pre-amplifier. This input capacity is in parallel with the detector capacity, and the larger the sum of these two, the smaller will be the dq/dt. It was thus necessary to choose as small a junction detector as possible, and an RCA type surface barrier detector with an area of 1 sq. mm. worked very well.

So that deuterons scattered from the generator would not give extra pulses, a foil of aluminum 300 μ gm/cm^2 was placed in front of the detector, and this was sufficient to stop the deuterons while not interfering significantly with the alpha particles.

Fig. 2

Circuit diagram of Time-of-Flight System Electronics

Legend:	T.P.O.	=	time-pick-off-unit
	T.P.C.	=	time to pulse-height converter
	Disc.	=	single channel analyser
	200 ns	=	delay line
	comp.	=	amplitude compensation for variation in rise time

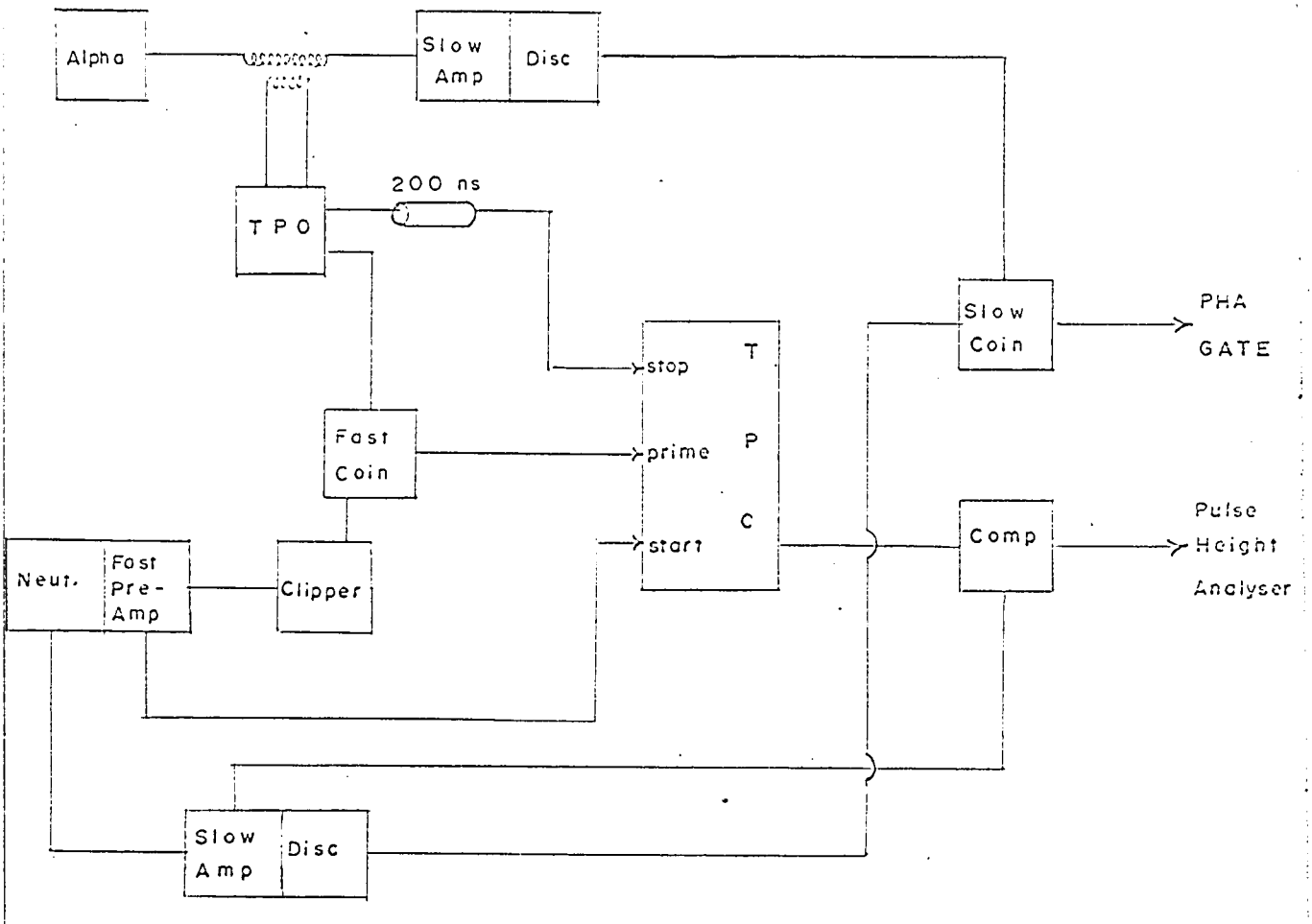
Alpha
Slow Amp
Disc
200 ns
T P O
Slow Coin
PHA GATE
stop
T
prime
P
C
start
Fast Coin
Neut.
Fast Pre-Amp
Clipper
Comp
Pulse Height Analyser
Slow Amp
Disc

The neutron generator (Texas Nuclear) employed an r.f. (100 k.c.) powered ion source. This was inside a 1/8" Aluminum dome at the back of the generator. In spite of all attemps to ground the generator and the electronics, a large pick-up, corresponding to 60% of the total possible bias on the time-pick-off unit, was encountered.

Attempts were made to shield the ion source with a steel cylinder, and to shield the pick-off unit with a metal box, but it was found that these were not effective due to the long lengths of a grounding wire(about 30 feet) necessary to join the electronics, generator and grounding post.

Mr. G. Cornish, Dr. W. J. MacDonald and the author then decided to build a d.c. powered ion source which could deliver up to 15 μ amps of deuterium ions.

The principle was to maintain a discharge in a tube filled with deuterium gas at low pressure (i.e. 1→10 mmHg). The negative electrode was to have a small hole in it, through which the beam could emerge into the neutron generator.

The size of the discharge tube is quite important in this application. The current that can be obtained is a function of the voltage across the electrodes, and the number of gas molecules between them. From zero to 5000 volts was available on the generator, and so the only variable remaining was the distance from cathode to anode. The effect known as "Gas Multiplication" is used to produce a working current. The electrons streaming from the cathode strike the molecules of the gas, causing them to ionize. The resulting positive ions are then accelerated toward the cathode, and some of them escape through a narrow canal drilled through the cathode leading out to the acceleration tube of the neutron generator.

If the molecular density of the gas is too high (i. e. the pressure is too great), two effects take place. The diameter of the canal must be relatively small in order to maintain this pressure against the vacuum in the rest of the system, and second, the electrons do not have enough space to accelerate to an energy where they can ionize the gas before colliding with another molecule.

On the other hand, should the pressure be too low, the current that one could obtain would be insufficient to perform the experiment. The only solution is to find the optimum distance between the electrodes for the voltage that one has available, and a pressure that one can maintain with a reasonable canal size.

Many combinations of tube length, and canal size were tried. The final working model consisted of a one inch glass tube with a plate shaped anode inserted in one end through a glass seal. The cathode was a 3/16 inch rod fitted into a hole in the other end of the tube, and the canal in the "rod" was drilled to a diameter of .031 inches. (See Fig. 3). The length of the discharge was 9.3 inches, and the voltage across the tube could be varied from the 3000 V necessary to strike, up to 5000 V.

The original canals were made from aluminum, but these were found to erode very rapidly and the D^2 pressure would be lost in about $2\frac{1}{2}$ days. Other materials were tried which included brass, stainless steel, cold rolled steel and finally'Inconel X' was found to last about 3 weeks provided the voltage did not exceed 4500 V.

The resulting loss of noise allowed the time-pick-off unit to be run at 6% of its total bias compared with the previous 60%.

Fig. 3

D. C. Powered Ion Source.

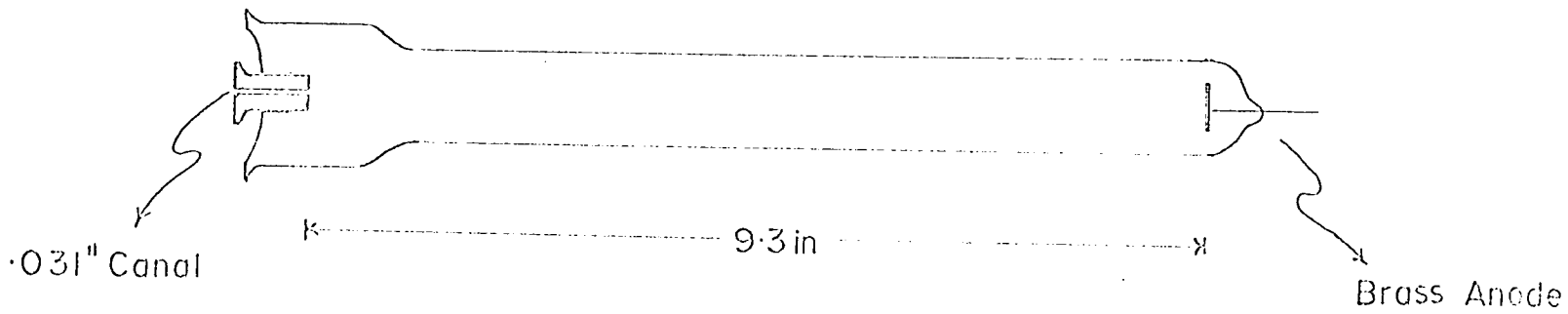

D·C· Powered Ion Source

The experimental set up is shown in Fig. 1. The O_2 target consisted of natural liquid oxygen (99.8% O^{16}) in a container made from styrofoam. The container was a "cup" 25 cm high by 7 cm diameter having a wall 1.5 cm thick, and the level of the liquid was maintained by a float operated valve coming from a 55 litre dewar. This container was placed in the beam defined by the associated particles striking the junction detector subtending 2.5° at half maximum intensity, and the amount of liquid O_2 actually involved in the scattering experiment was slightly smaller than the dimensions given above.

The neutron detector was an NE 102 slab 4 in. by 2 in. by 12 in. mounted on an RCA 7046 photo-multiplier tube. This slab was placed such that its long axis was inclined at 65° to the incoming beam, the photo-multiplier end being more distant from the target. This was to compensate for the time required for the light to travel from the far end of the slab to the photo-multiplier.

This arrangement was shielded from neutrons scattered from the floor and walls by a "castle" made from blocks of paraffin soaked wood sandwiched in steel. The castle had a long open side to it such that the detector could just "see" the oxygen target. The front of this opening was protected from direct neutrons by a brass shadow bar 12 in. long by $3\frac{1}{2}$ in. diameter.

The angular correlation between the target, beam and neutron detector were measured by a system of protractors mounted to the generator, acting as a support for the styrofoam dewar. The angular resolution was about 5°.

The coincidence units were utilized in a more efficient manner than is described in [1], by demanding a fast coincidence between the time-pick-off (T.P.O.) output and the fast neutron channel, and using this to prime the time-to-pulse-height converter (Fig. 2). A slow coincidence (1 μs) was demanded between the outputs of the discriminators in the two slow channels, and this was used to gate the pulse height analyser.

The fast neutron channel carried pulses which were generated by having the photomultiplier signal saturate a pre-amplifier. This resulted in a "square wave" whose duration was proportional to the input pulse height. They could last anywhere between 15 and 150 n sec. A clipping device held all pulses to 15 n sec. before demanding fast coincidence with the T.P.O. output. Because these pulses were so short, compensation had to be made for the flying time of the neutrons, the processing time of the pulses through the clipper, T.P.O. and fast pre-amplifier. This was done by inserting various lengths of cable between the stages until the pulses "lined up" properly on a fast oscilloscope. Furthermore, the pulses used to start the time to pulse height converter had to be delayed long enough so as not to precede the prime pulses, but not so long as to have them there when the stop pulse arrived. Finally the slow coincidence output had to coincide with the pulse height analyser input so that the gate would remain open only for the correct pulse. The oscilloscope used for this alignment had a rise time of 1.5 n sec.

Two methods were used to calibrate the system. The first was to place the neutron detector directly in the coincidence beam. Two distinct peaks could be seen, one corresponding to γ -rays the other to 14.1 MeV neutrons. The time required for

each of these to traverse the known flight path was calculated, and the time difference related to the number of channels between the peaks.

The second method was to move the neutron detector back and forth a known distance (usually $1\frac{1}{2}$ metres) in the coincidence beam, and note the relative displacement of the two peaks.

A bias was set on the neutron discriminator corresponding to the .6 MeV γ peak in Cs^{137}, with an equivalent neutron energy of $\approx$2 MeV. With this bias, the time resolution, as given by the full width at half maximum of the 14.1 MeV peak was 1.2 n sec. This meant that one could distinguish neutrons separated by .5 MeV or greater.

Fig. 4 shows the time spectra obtained with the original equipment, while Fig. 5 shows spectra obtained with the improved version. Such spectra as shown in Fig. 5 were taken at 16 angles between 20° and 150°. As can be seen, the levels lying near -7 MeV are clearly distinguished from those lying near -6 MeV, but the individual structure is not apparent.

The differential scattering cross-sections for the elastic, -6 MeV and -7 MeV levels were computed. The elastic data agreed perfectly with a previous experiment performed by Dr. MacDonald. Corrections had been made on this original data to account for; effects on the incident and scattered neutrons by the oxygen in the target, multiple scattering events, and finite angular resolution. The latter two were accomplished using a Monte Carlo program developed by Mr. C. Glavina[2]. These corrections were about 10% or less except near the relative minima, where they were of the order of 25%.

Fig. 4

Time spectrum of Neutrons scattered by liquid oxygen.

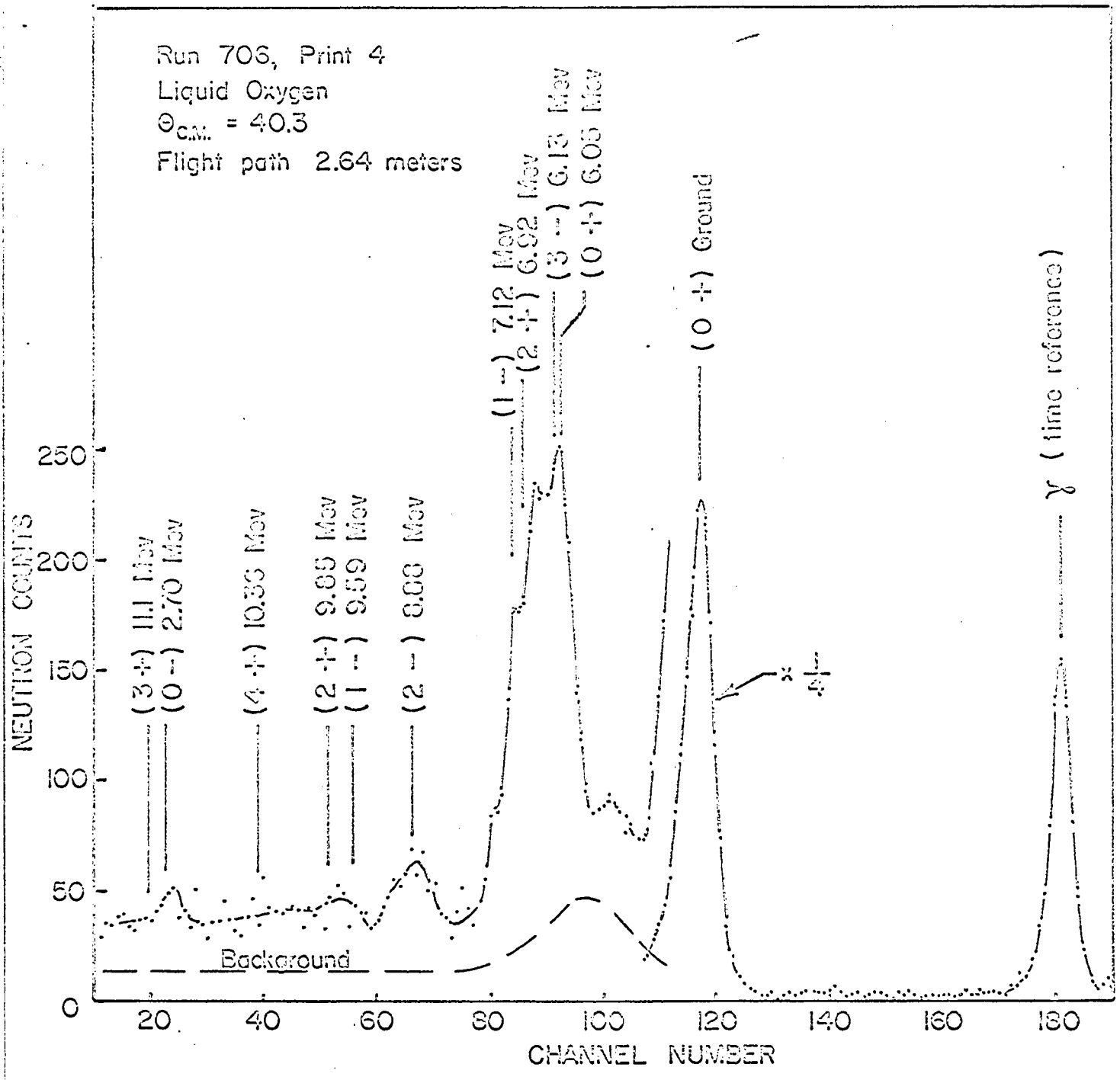

Time spectrum of Neutrons scattered by liquid oxygen.

Fig. 5

Time of flight spectra of neutrons scattered from liquid Oxygen.

a) $\theta_1 = 41^\circ$ Path length = 230 cm
10 ch = 4.7 ns.

b) $\theta_1 = 130^\circ$ Path length = 230 cm
10 ch = 4.7 ns.

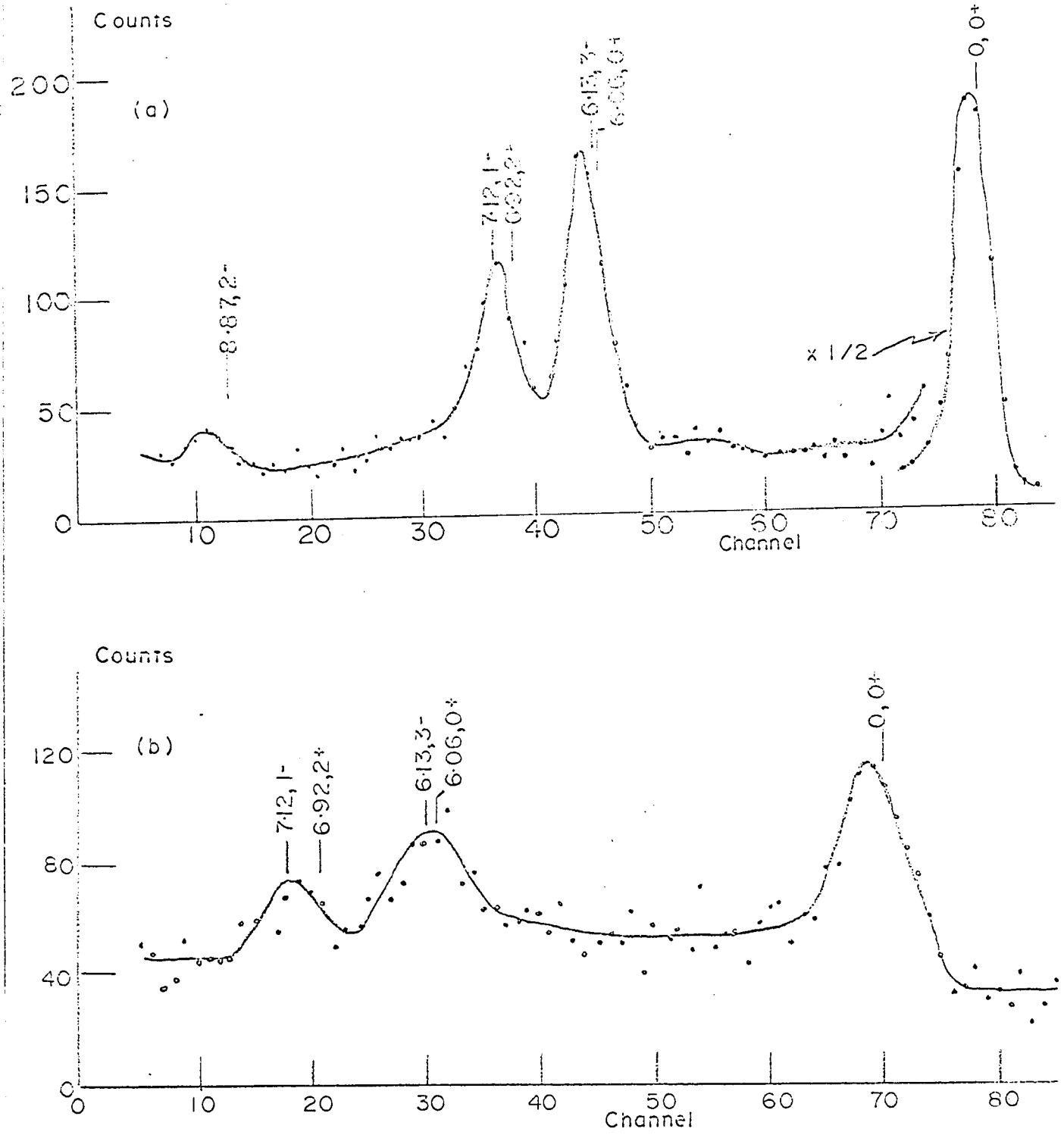
Counts
(a)
200
150
100
50
0
8·87,2-
7·12,1-
6·92,2+
6·13,3-
6·06,0+
0,0+
x 1/2
10
20
30
40
50
60
70
80
Channel
Counts
(b)
120
80
40
0
7·12,1-
6·92,2+
6·13,3-
6·06,0+
0,0+
10
20
30
40
50
60
70
80
Channel

Figs. 6 and 7 show the differential cross-sections calculated from the data. Since the elastic data agreed so well with the original work, it was decided not to perform the Monte Carlo corrections on them, and Fig. 6 shows the points taken by Dr. MacDonald as representing the elastic curve.

By drawing a smooth curve through the experimental points, and doing a numerical integration, the total cross-section for the individual reactions were obtained. For the elastic peak, $\sigma = 1.07 \pm .25$ b (10^{-24} cm^2). The -6.1 MeV peak has a $\sigma = 96 \pm 10$ mb, and the -7 MeV peak has a $\sigma = 58 \pm 7$ mb.

The errors indicated by the error bars represent only the errors due to statistics and background subtraction. For the elastic data these uncertainties were smaller than the circles around the points. In addition to the errors indicated, there was an uncertainty in the relative cross-section for each point of 5% or less due to variations in the sample position, neutron beam cross-sectional area, and errors in the Monte Carlo Corrections.

Conclusions.

The T.O.F. system described above is quite satisfactory for measuring states separated by ≈ 1 MeV for incident energies up to about 20 MeV. A resolution of 1.2 n sec. was achieved, but to improve this significantly, a technological breakthrough in neutron detectors would be necessary.

If the size of the detector is reduced, so as to make the error in detection time less, the efficiency drops, and one encounters problems in long time stability of the electronics. As it was, running times of up to $2\frac{1}{2}$ days were necessary to get good statistics and a more elaborate set-up including temperature controlled rooms would be necessary to go much further.

Fig. 6.

Differential Cross-Sections of Elasticly Scattered and Q = -6 MeV Neutrons.

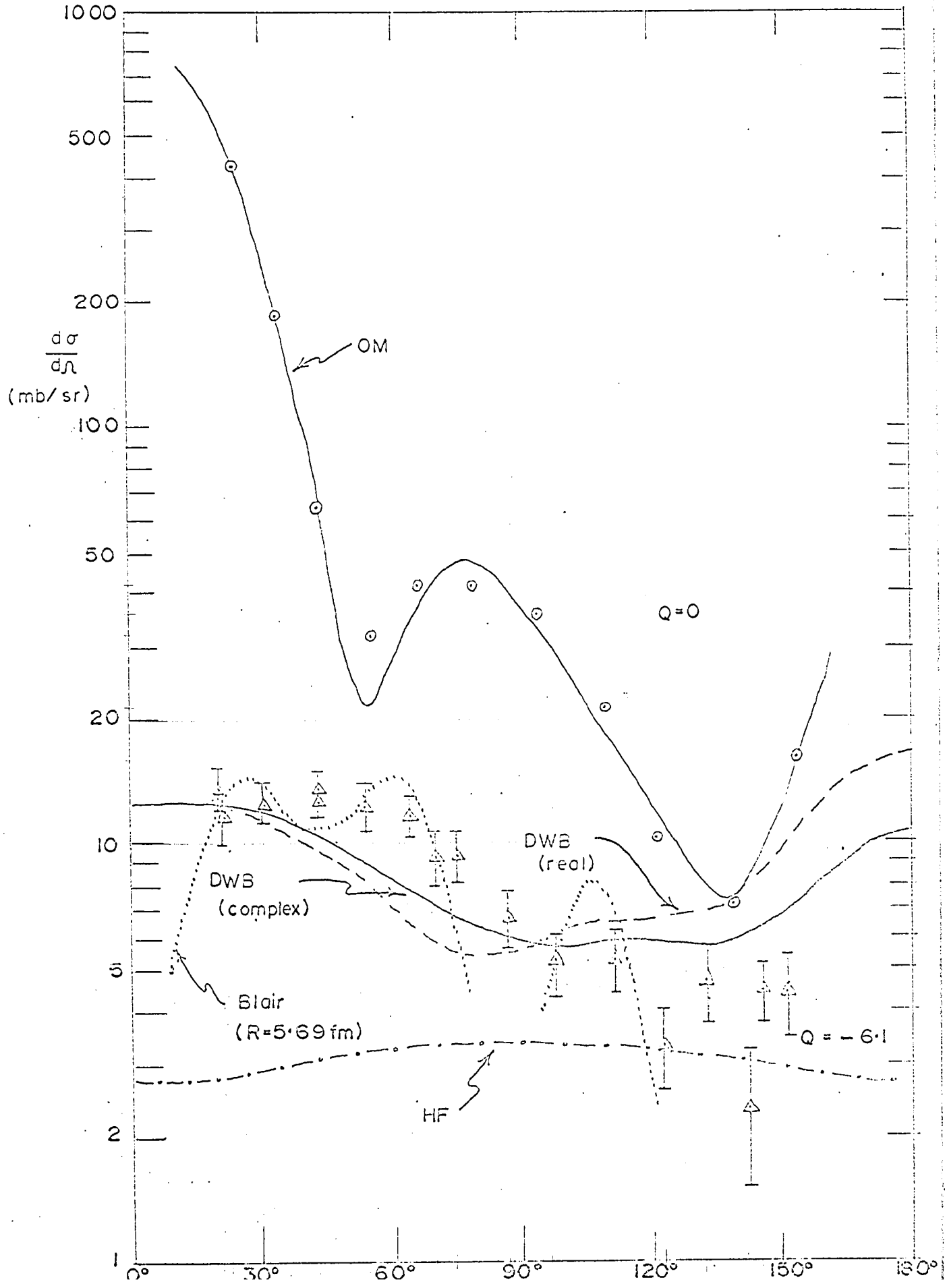
1000
500
200
100
50
20
10
5
2
1
dσ/dΩ
(mb/sr)
OM
Q=0
DWB
(real)
DWB
(complex)
Blair
(R=5·69 fm)
HF
Q = −6·1
0°
30°
60°
90°
120°
150°
180°

Fig. 7.

Differential cross-section of scattered neutrons corresponding to Q = -7.1 MeV.

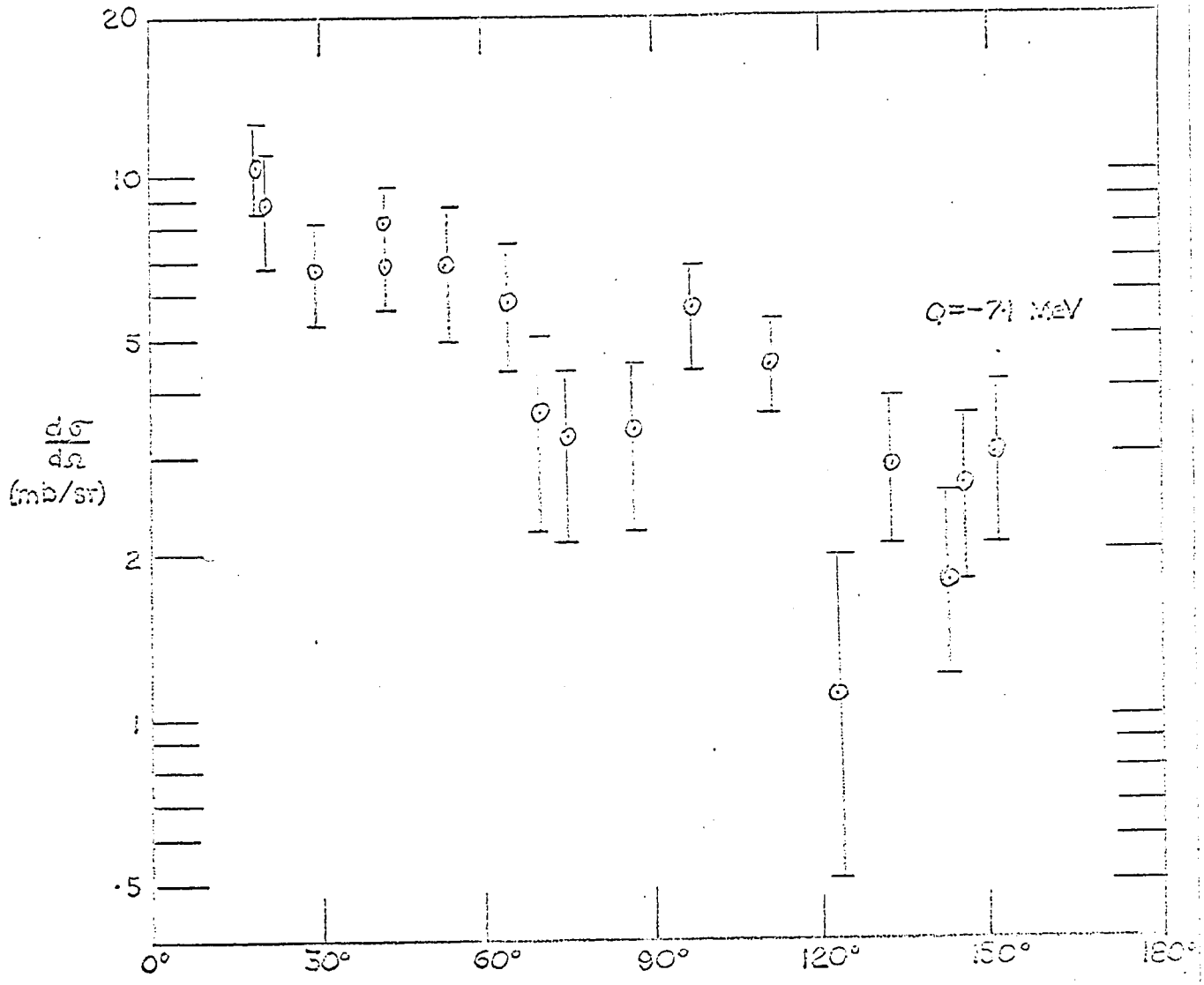
20
10
5
2
1
·5
dσ/dΩ (mb/sr)
Q=-7.1 MeV
0°
30°
60°
90°
120°
150°
180°

The background and pile up problems cause trouble if the neutron flux is increased, and a beam chopper or buncher could reduce at least the former of these considerably, especially if the walls and floor are well removed from the experimental area.

Appendix C shows calculations done to find what the optimum operating sizes of detector and flight path should be.

Appendix A is taken from a paper by W. J. MacDonald, J. M. Robson and R. Malcolm to be published. This was done since the author's main concern with the experiment was with the setting up and running of the equipment, and performing a few of the calculations. The theoretical interpretation of the results was the work of the other two authors of the paper.

PART II

Introduction.

The problem of shielding from fast neutrons is important if only for reasons of the health of people near fast neutron sources, and yet not much is known about how a neutron beam is attenuated in shielding material. Currently, the amount of shielding is specified by measuring the amount of neutrons from the type of source in question which traverse the shielding material and strike a block of paraffin containing a counter which is sensitive to thermal neutrons. The protons in the paraffin slow down the neutrons to allow them to be easily detected, and the cross-section of such a counter can be related to that of living tissue. It is felt however, that more efficient means of shielding from neutrons than is presently used could be devised if the attenuation mechanism was well understood.

The lack of experimental work on this problem is due to the trouble one encounters when trying to build a system which will not only record the presence of neutrons, but also gives an indication of their energy. Such spectrometers have been built and can operate up to about 20 MeV, and one is described in a report by J. M. Robson and C. Glavina[1].

The principle employed was to measure the time required by the scattered neutrons to traverse a known distance before being detected. Such a time-of-flight system is also described in the other part of this thesis.

There is a major disadvantage to using a time-of-flight system for work with shielding materials. Unless the target is fairly thin ($\leq$ 10 cm) a large error results from not knowing the location at which the scattering event occurred, or whether the neutron observed had undergone a single or multiple scattering events before being detected.

The present work is a continuation of the work mentioned above[1]. It was hoped that some device could be found which was not prohibitively expensive, and yet could be used as a neutron spectrometer for neutrons of up to 14 MeV of energy. If, and when such a device was obtained, the experiments done on Carbon[1] would be repeated as a check on the apparatus. The attenuation of neutrons through a wall of carbon would then be measured, and a Monte Carlo program to predict these results checked.

The final stage would be to test concrete of various compositions and configurations, and observe whether the results can be predicted on the basis of present theory.

There are a few qualifications that a suitable spectrometer device must have. It should not be too large, or the angular resolution will be poor. It should have a reasonable efficiency so that good statistics can be compiled without worry as to the stability of the associated electronics. The resolution, measured as the full width at half maximum of monoenergetic neutrons, divided by the energy, should be no greater than 15% (i. e. about 1 MeV at 14 MeV).

The present work describes the search for a suitable detector. This task proved to be considerably more difficult than was

first anticipated, since the most promising device found required a long time to manufacture and deliver, and when it was received it proved to be defective.

Experimental Details.

The first counter to be tested was a "Texas Nuclear Texlium" type 319 He^3 Krypton activated proportional counter. It was made of 1 inch diameter stainless steel tubing, 1/32 in. thick, with an active length of 6 in. It contained 4 atmospheres of He^3 and 2 atmospheres of Krypton. The Krypton, with its higher Z, reduces the path length of the charged particles in the gas, and is added to keep the particles from loosing too much energy to the walls of the counter. The reaction that this counter is based on is $He^3 + n \rightarrow p + T + 764$ KeV.

The counter was calibrated by placing it in an 8"x8"x12" block of paraffin which had a Ra-Be neutron source in it. The thermal neutrons from this arrangement gave a good sharp peak. A Texas Nuclear model H150 neutron generator was used to generate 2.5 MeV or 14 MeV neutrons. Figs. 1 and 2 show the results of bombarding the "Texlium" detector with 2.5 MeV neutrons. The peak corresponding to thermal neutrons arises from neutrons scattered from the walls and floor of the lab, and is so prominent because the cross section of He^3 for thermal neutrons is 5000 b while for 2.5 MeV neutrons it is about .6 b. The diagram also indicates where the 2.5 MeV neutrons should occur. The first figure shows the spectrum obtained with the detector pointed end-on towards the neutron source, while the second shows the same counting time, but with a 1/16 inch thick Cd sleeve about the detector.

Fig. 1.

2.5 MeV neutrons seen with a "Texlium" proportional counter.

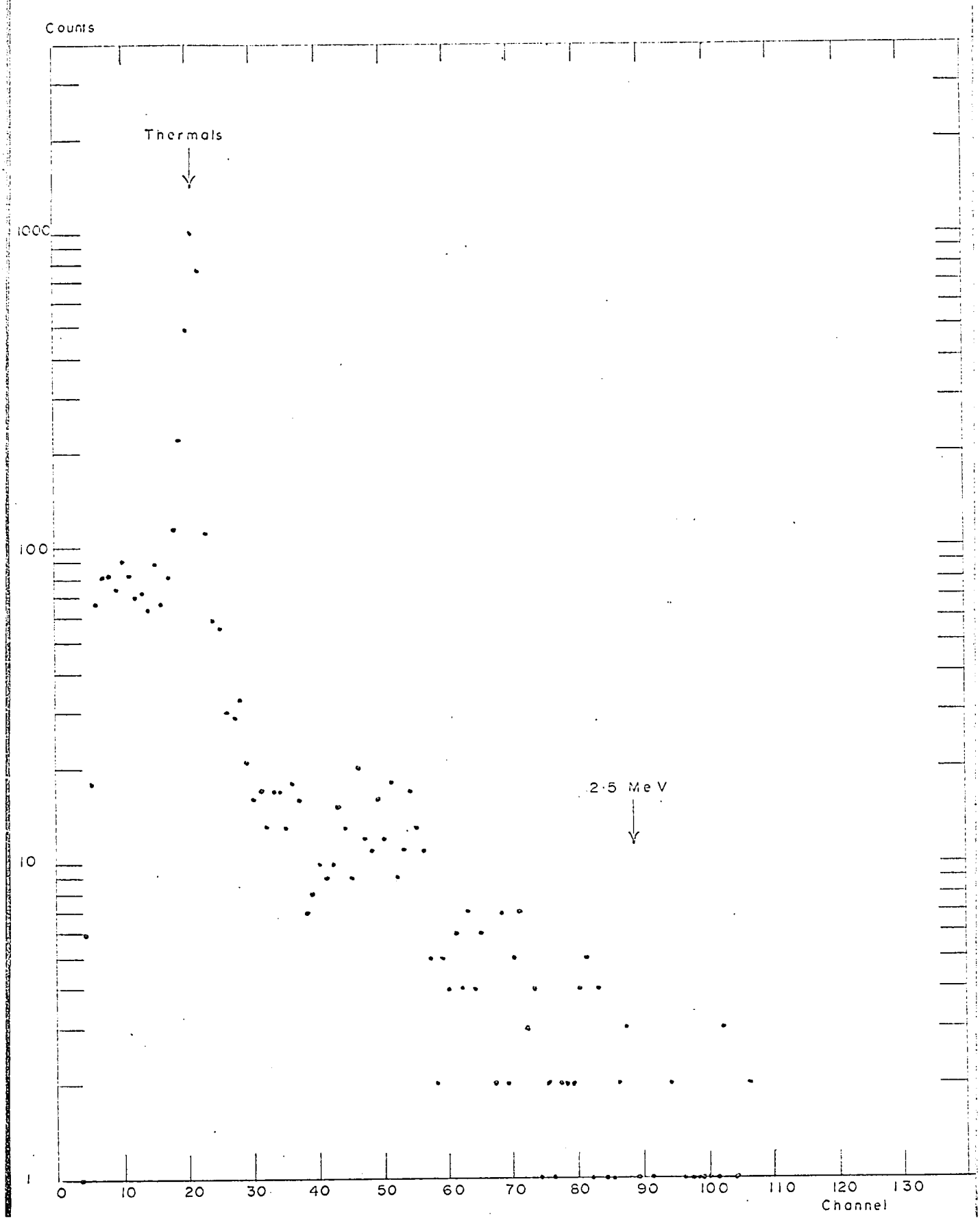
Counts
Thermals
1000
100
10
1
2·5 MeV
0
10
20
30
40
50
60
70
80
90
100
110
120
130
Channel

Fig. 2.

2.5 MeV neutrons seen with a "Texlium" proportional counter surrounded by 1/16 inch of Cadmium.

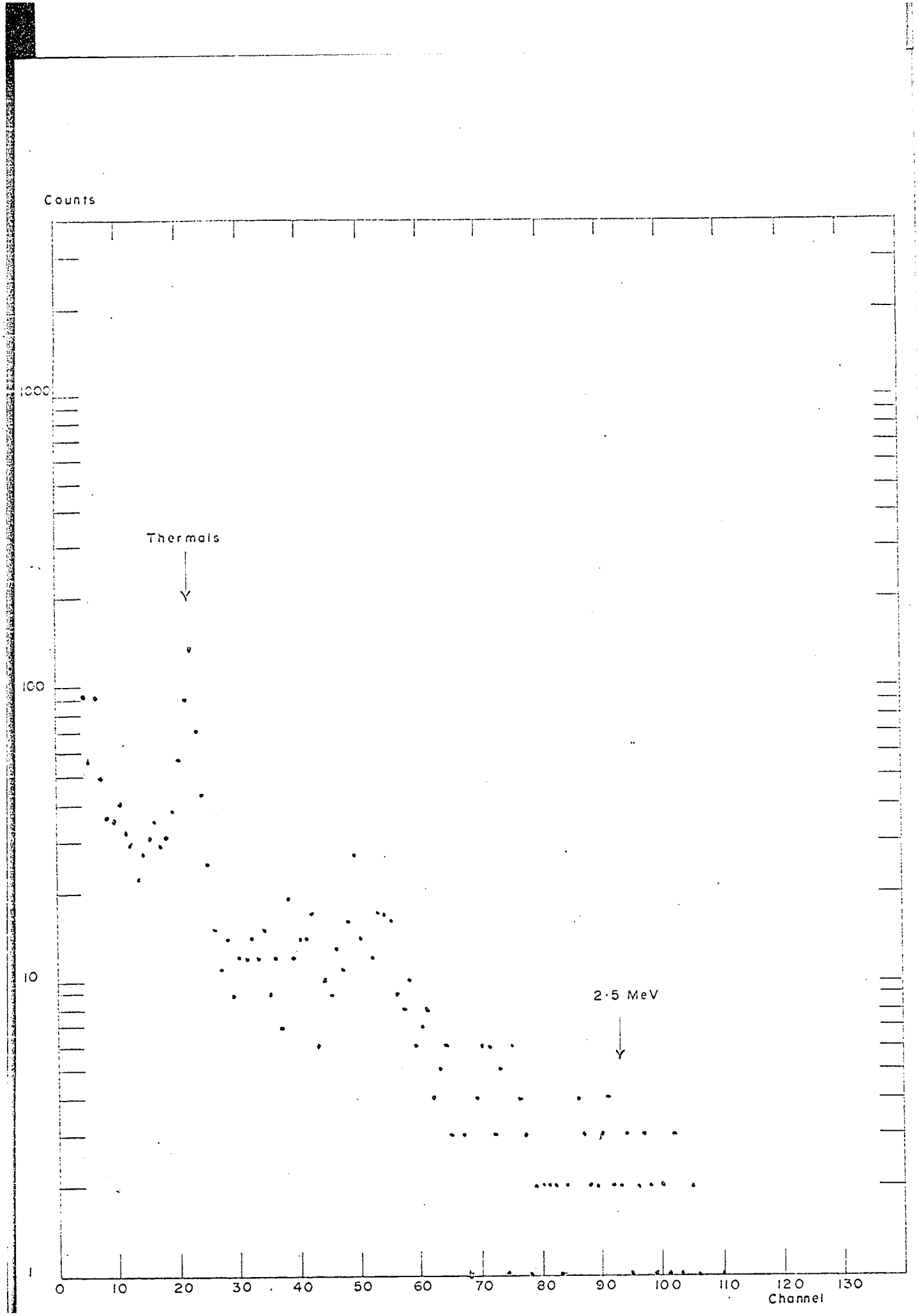
Counts
1000
100
10
1
Thermals
2·5 MeV
0
10
20
30
40
50
60
70
80
90
100
110
120
130
Channel

Cd. has a high capture cross-section for thermal neutrons, while being relatively transparent to energetic neutrons.

As would be expected, in view of the response to 2.5 MeV neutrons, the results with 14 MeV neutrons were completely negative. Nothing even resembling a peak could be found.

Appendix A shows a calculation done, assuming 2.5 MeV neutrons incident on the detector, and which indicates that only about 25% of the neutrons which react with the gas in the counter will give their full energy towards making an electrical pulse. The remaining 75% lose at least some part of their energy to the walls of the counter, and the resulting pulse does not have enough energy to be counted as a 2.5 MeV particle. This calculation did not take into account the higher cross-section of the counter for neutrons of lower energies, since the energy distribution of the neutrons in the room was not known. However it can be seen that this could only worsen the effect described.

A BF^3 proportional counter of the same dimensions was used to check the electronics employed with the "Texlium" detector. BF^3 counters are quite common, and their response is well known. The electronics proved to be quite good.

In order to check that γ -rays were not giving trouble, the "Texlium" detector was operated while resting on a 1 m curie Co^{60} source which has two γ -rays at about 1 MeV. Under these conditions, the counter was still able to detect thermal neutrons generated 25 feet away with no appreciable loss of resolution.

A large BF^3 proportional counter was next set up for study. It was 65 cm long by 5 cm diameter, and contained 1 atm

of BF^3. It was surrounded by 1/16 in. of Cadmium sheeting, to absorb most of the thermal neutrons generated in the room, since $Boron^{10}$ too has a large reaction cross-section for thermal compared with energetic neutrons. When subjected to 2.5 MeV neutrons, it gave a broad peak, whose resolution was so poor that it overlapped the peak corresponding to thermal neutrons. The reaction used by this counter is $B^{10} + n \rightarrow \alpha + Li^7 + 225$ KeV. The low Q of this reaction, the relatively low cross-section at high energies (.6 b at 1 MeV compared with 3800 b at thermal energies), and the large size which results in poor angular resolution would indicate that this counter is not satisfactory for the intended experiment. The low Q means that competing reactions in the counter can give rise to pulses which cannot be distinguished from those arising from neutrons. Some of these reactions are;

Photo electric effect and compton scattering of γ-rays.

$Cu^{63}(n,p)\ Ni^{63} + .7$ MeV

$Cu^{63}(n,\ )\ Co^{60} + 1.7$ MeV

Cu^{63} constitutes roughly 70% of the brass walls of the large BF^3 counter, and the last reaction has a cross-section of 23 mb (compared with about .2 b for B^{10} at 2.5 MeV).

The data from this counter showed an exponential tail which extended beyond the peak from the 2.5 MeV neutrons, and this was attributed to the above reactions. A run using 14 MeV neutrons gave negative results.

The next device to be tested was a Li^6 loaded glass phosphor (NE 902), approximately $2\frac{1}{2}$ inches in diameter by $\frac{1}{2}$ inch thick. This was mounted on an RCA 6342A photo-multiplier, which fed a Victoreen transistorized pre-amplifier, which in turn drove a Victoreen 200 channel Pulse Height Analyser.

The system was mounted in a beaker in such a way that various combinations of shielding material could be tried around the scintillator (Fig. 3).

The dynamic range of the pre-amplifier was such that the photo-multiplier had to be operated at 950 volts instead of the usual 1250, however the relative noise level was low, and the low voltage did not pose much of a problem.

Various runs at thermal energies, 2.5 MeV and 14 MeV were done trying different shielding combinations and background subtraction with the generator off.

Fig. 4 shows the results obtained with this system. From right to left, are; Thermal neutrons from Ra-Be in paraffin, 2.5 MeV neutrons, 2.5 MeV neutrons with the background,while the generator was off, subtracted, and 14 MeV neutrons with the background subtracted. As may be seen, the 2.5 MeV neutrons are barely discernable at channel No. 23, while nothing is visible around channel 59 which corresponds to 14 MeV neutrons in the last diagram.

The gain of the system was increased, and the scintillator irradiated with thermal neutrons again. Fig. 5 shows the results, and a resolution (full width at half max divided by channel number) of 22% was obtained.

Different combinations of Cadmium and Boron Carbide shielding were tried, and Fig. 6 shows the results of 2.5 MeV neutrons seen with Cd and B_4C around the scintillator. The resolution is only 50% here, which may be explained by the fact that the $Li^6 (n, \alpha) H^3$ reaction has a resonance in its cross section which is 3 times higher at this energy than for lower energies down to several hundred KeV^2. This means that quite a wide range of energies might show up in the

Fig. 3.

Experimental arrangement for studying a Li^6 loaded glass scintillator. The inner cylinder was made from Cadmium, but could be replaced with a similar one of cardboard.

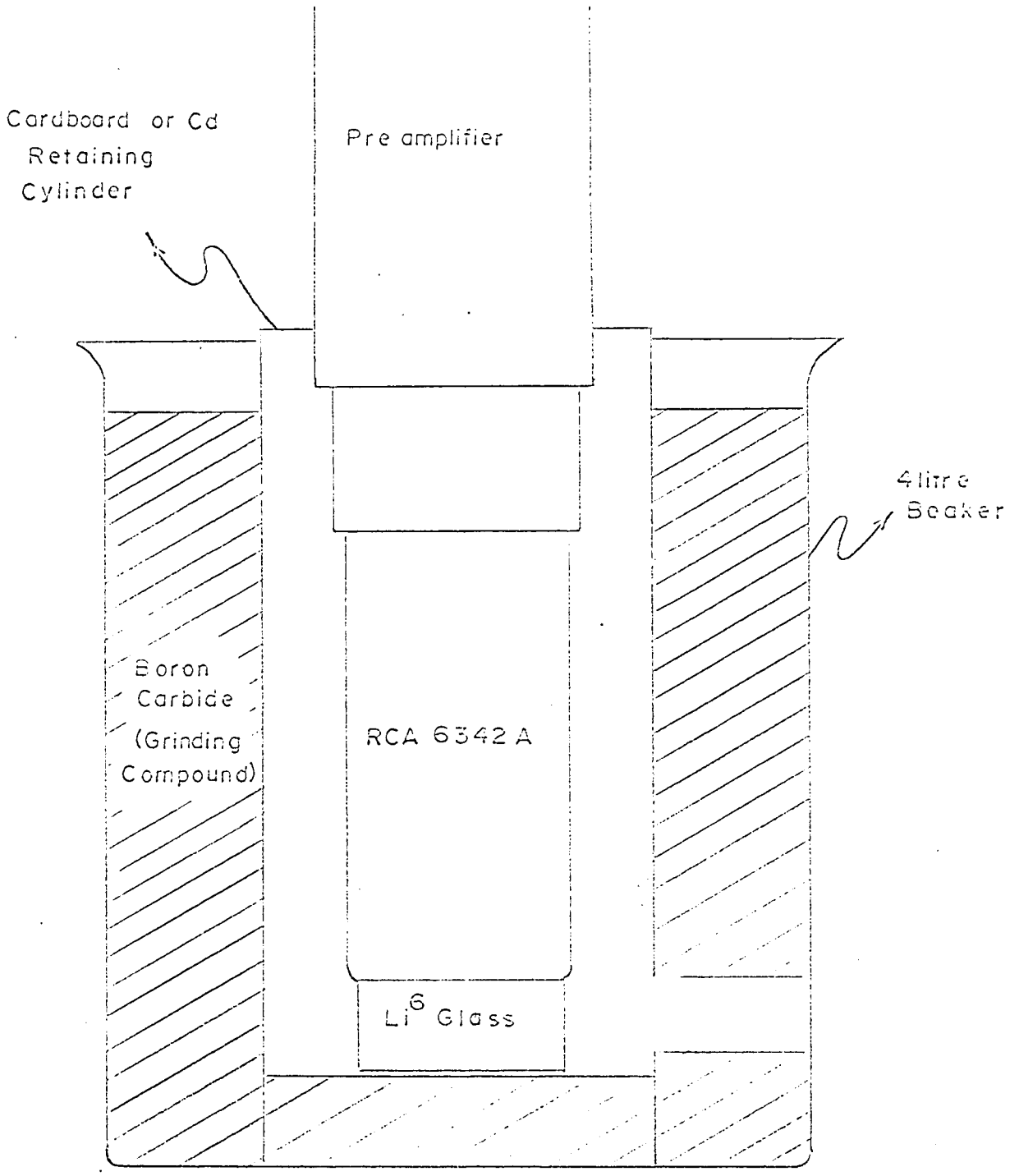
Cardboard or Cd
Retaining
Cylinder
Pre amplifier
4 litre
Beaker
Boron
Carbide
(Grinding
Compound)
RCA 6342 A
Li 6 Glass

Fig. 4.

A. Response of Li^6 loaded glass scintillator to thermal neutrons.

B. Response to 2.5 MeV neutrons.

C. Response to 2.5 MeV neutrons with the background (generator off) subtracted.

D. Response to 14 MeV neutrons, background subtracted.

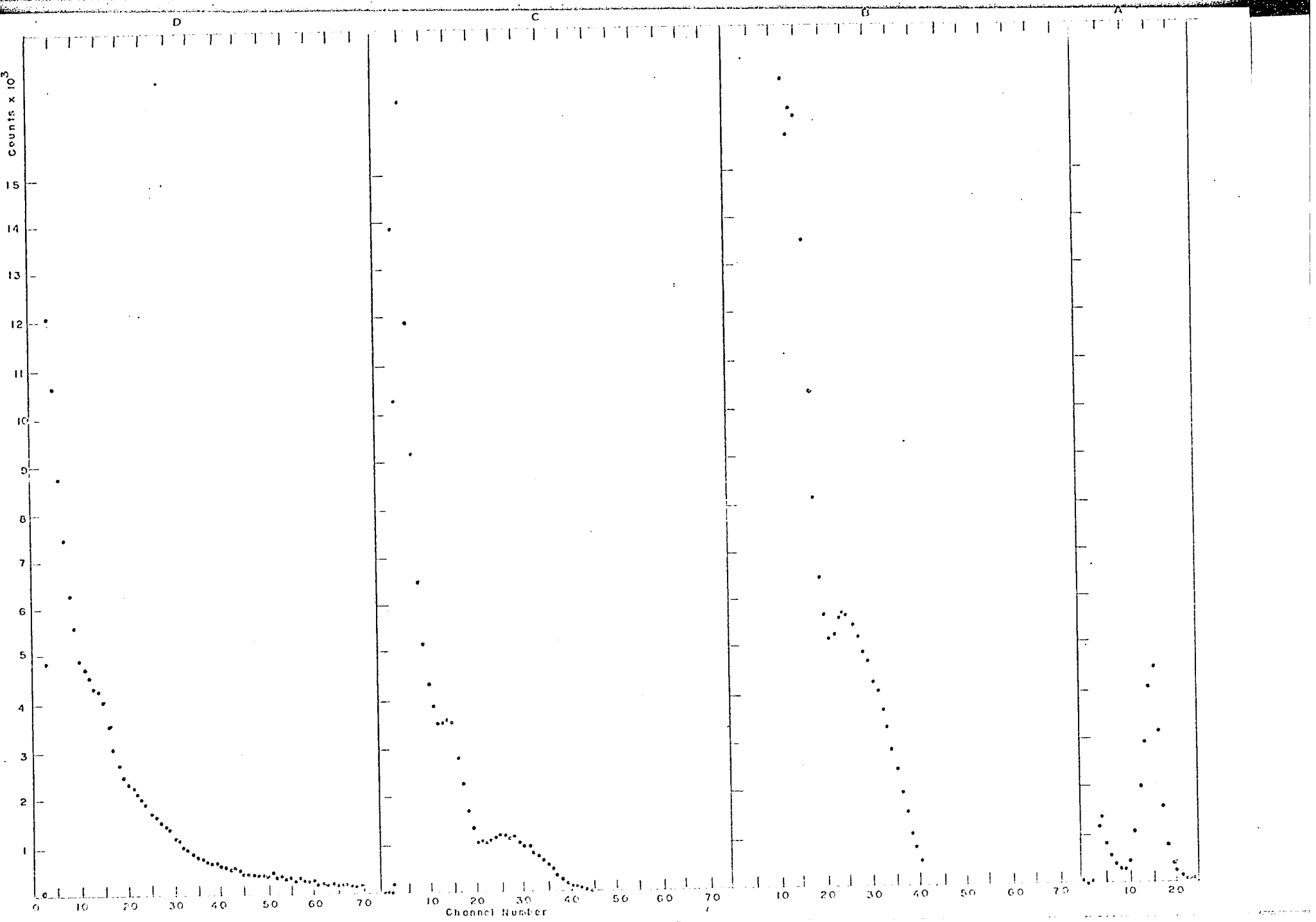
D
C
B
A
Counts x 10^3
15
14
13
12
11
10
9
8
7
6
5
4
3
2
1
0
10
20
30
40
50
60
70
Channel Number

Fig. 5.

Thermal neutrons as seen with Li^6 loaded glass.
The resolution is 22%.

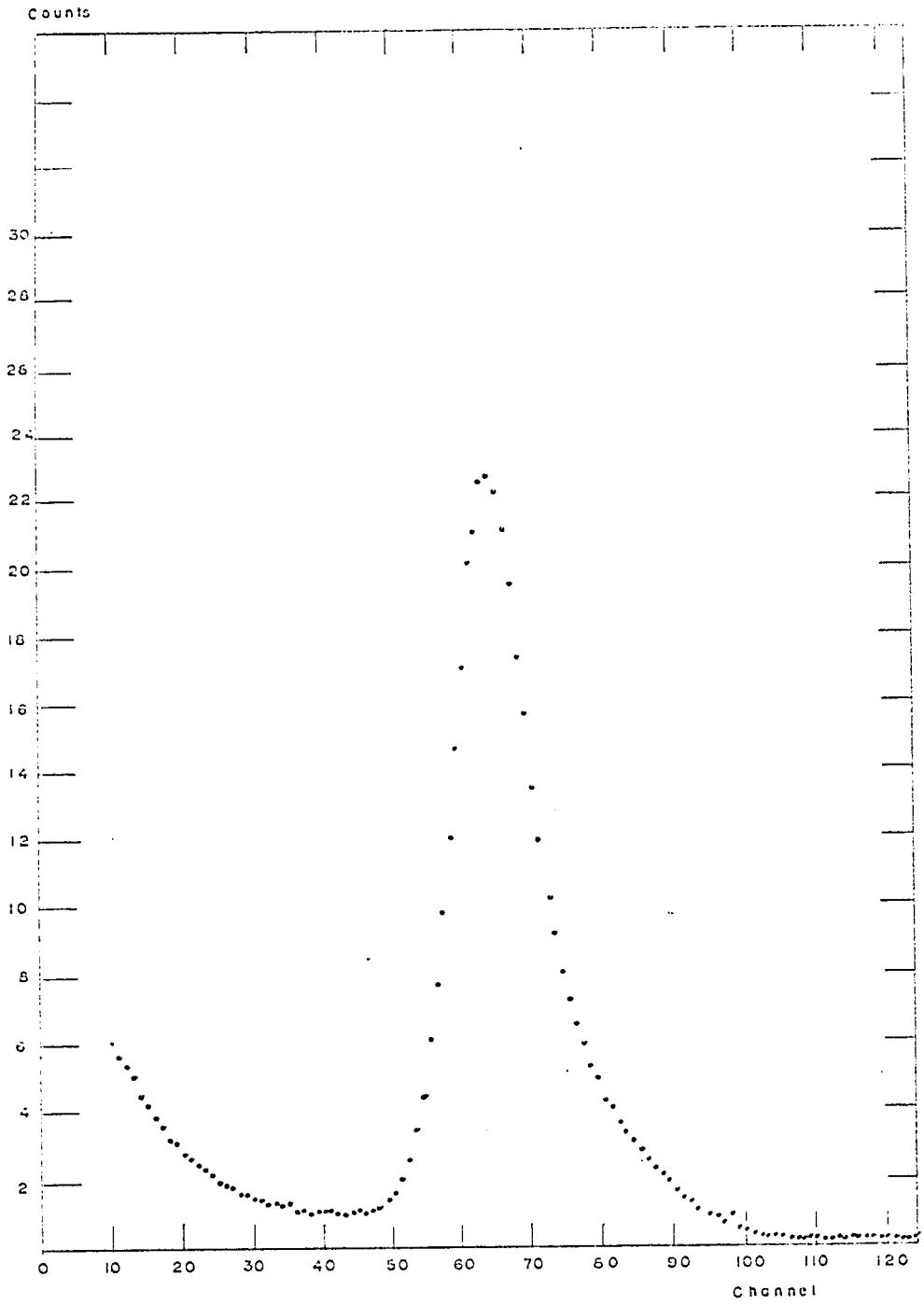
Counts
30
28
26
24
22
20
18
16
14
12
10
8
6
4
2
0
10
20
30
40
50
60
70
80
90
100
110
120
Channel

Fig. 6.

2.5 MeV neutrons seen with Li^6 loaded glass, surrounded by B_4C and Cd. The resolution is 50%.

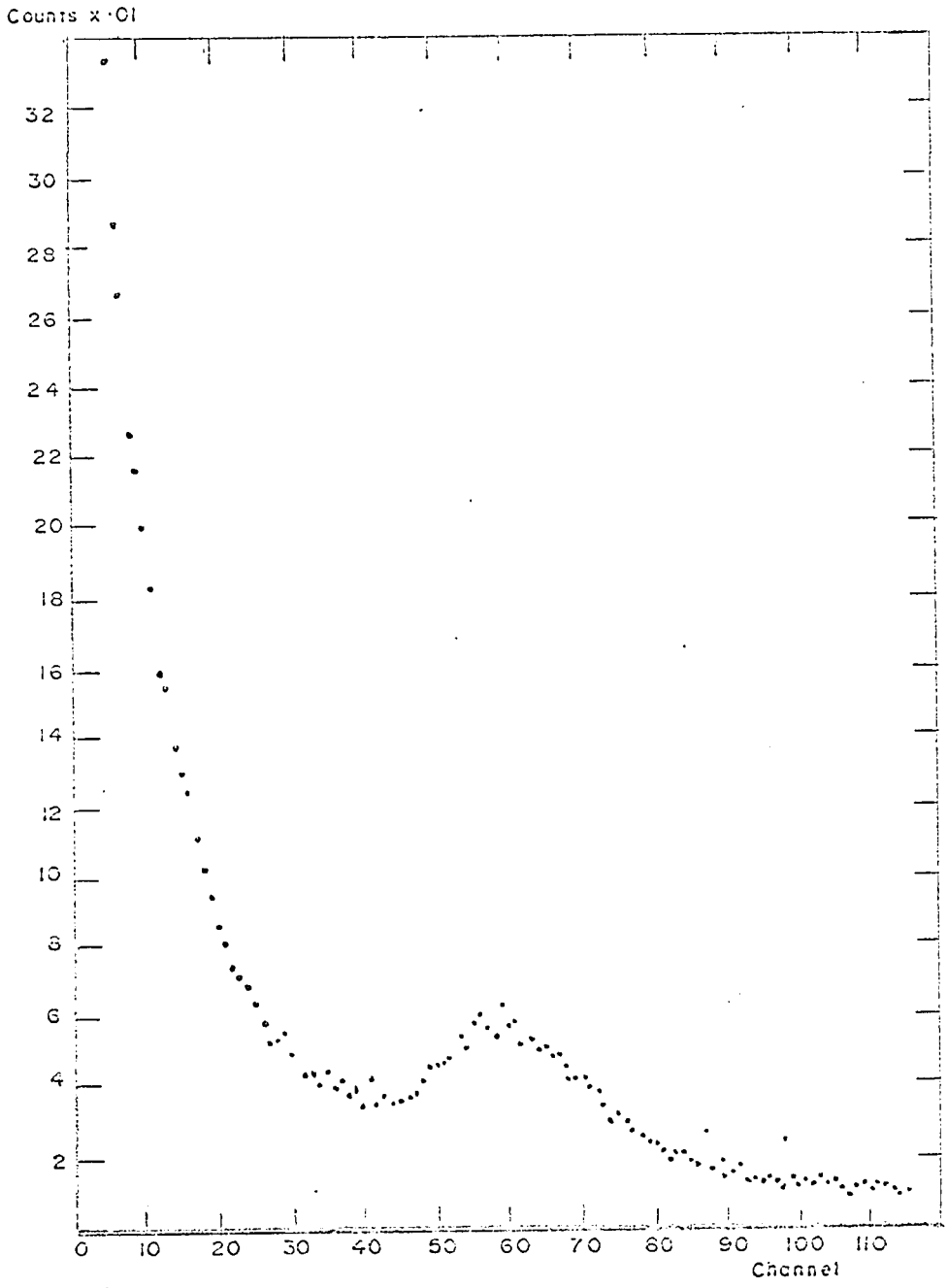
Counts x ·01
32
30
28
26
24
22
20
18
16
14
12
10
8
6
4
2
0
10
20
30
40
50
60
70
80
90
100
110
Channel

Fig. 7.

Time-of-Flight Apparatus used to select only 14 MeV neutrons being detected by Li^6 loaded glass.

Fast-slow	-	fast and slow channels of associated particle detector pre-amplifier.
COIN.	-	coincidence.
INV.	-	inverter.
TAC	-	Time-to-Amplitude Converter.
SCA	-	Single channel analyser.

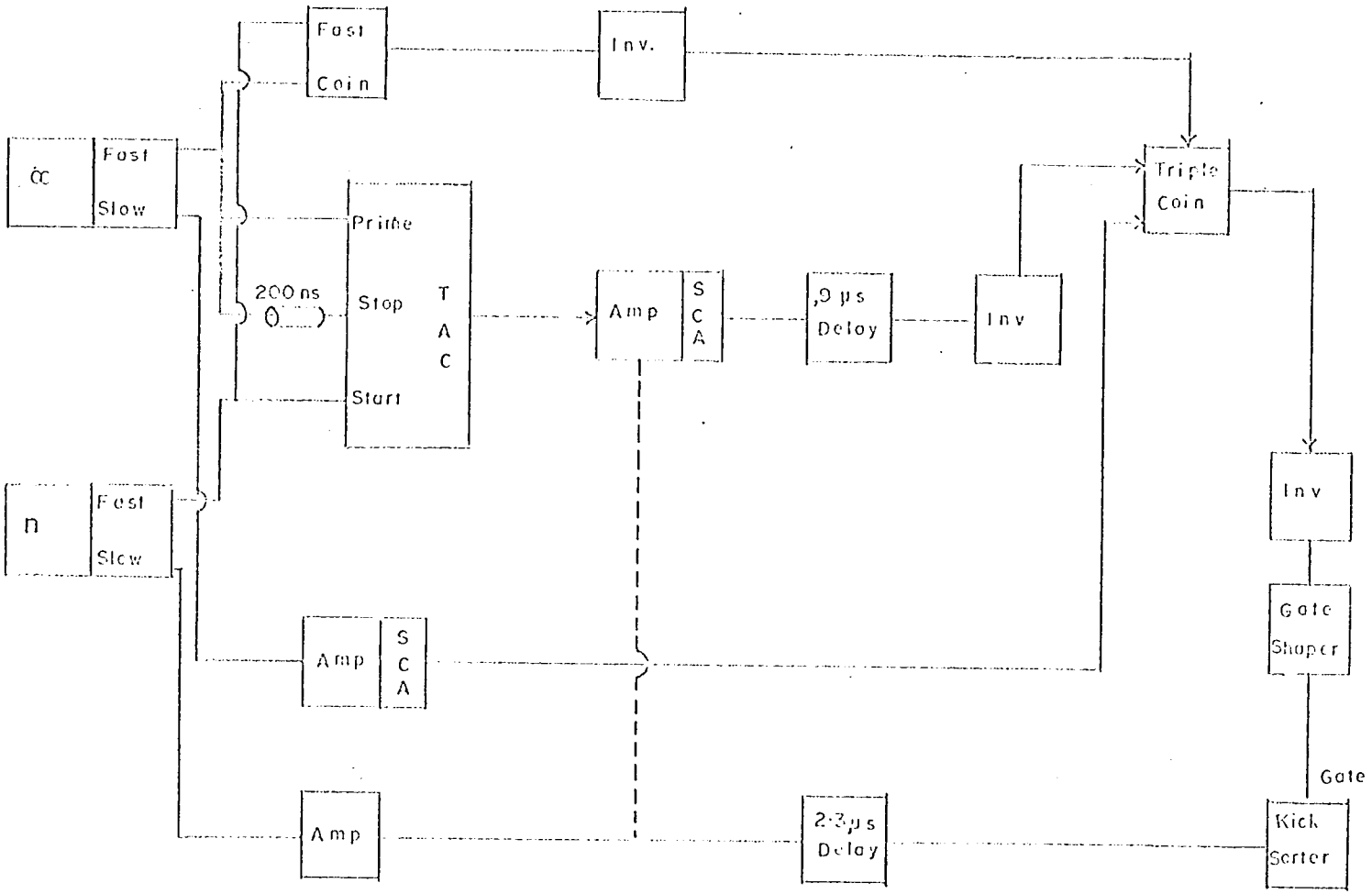
Fast
Coin
Inv.
Triple
Coin
α
Fast
Slow
Prime
200 ns
Stop
T
A
C
Start
Amp
S
C
A
,9 μs
Delay
Inv
n
Fast
Slow
Inv
Gate
Shaper
Amp
S
C
A
Gate
Amp
2·3 μs
Delay
Kick
Sorter

peak, due to neutrons scattered from the walls and floor, as well as the 2.5 MeV neutrons from the generator.

A time-of-flight system designed and built by Dr. W. J. MacDonald, and described in the other part of this thesis, was used to select only those events which corresponded to a 14 MeV neutron striking the scintillator. Fig. 7 shows a block diagram of the electronics used in this apparatus, and the block labelled n, fast and slow, was the phosphor-photo-multiplier-pre-amplifier used in this experiment.

By feeding the output of the TAC through an amplifier and into the kick-sorter, the entire spectrum of neutrons and γ -rays in the coincidence beam could be observed. A single-channel-analyser was used to gate the system so that only events corresponding to 14 MeV neutrons would be processed.

Fig. 8 shows the spectrum obtained with this arrangement. Thermal neutrons occur at channel No. 25, while those pulses corresponding to 14 MeV neutrons should occur at channel No. 98. Besides the fact that nothing is apparent corresponding to 14 MeV neutrons, two curious effects are noted; a long exponential tail extending well beyond channel 98, and a peak at what corresponds to 2.5 MeV. The chances that spurious 2.5 MeV neutrons would be recorded, despite their higher cross-section is extremely small because of the time-of-flight apparatus.

F. W. K. Firk et al[3] show that the electron efficiency in this detector is 1.6 times that of the products of the neutron reaction, and so the peak at channel 40 could be due to 4.5 MeV γ-rays, of which there are many in the room due to neutron capture processes in the

walls. Those events at channel 100 could correspond to 12 MeV γ -rays which is not unreasonable, since the phosphor has a diameter of $2\frac{1}{2}$ inches.

The obvious way to check this would be to examine the spectrum obtained from a similar Li^7 loaded glass, which is relatively insensitive to neutrons, but such a glass was not available at the time of the experiment.

Consider what happens to a neutron when it enters the scintillator. Besides passing right through unnoticed, it can interact with any of the constituents of the glass. The lighter the nucleus, the more energy it will carry away with it, and since it is very likely to leave electrons behind, it will create a scintillation just as any other charged particle. If the incident neutrons have 14 MeV of energy, then the lightest nucleus with which an elastic scattering could take place is Li^6, which would recoil with 7 MeV of energy. By comparing the elastic scattering cross-section with the capture cross-section one can conclude that there will be roughly 7 times as many such scattering events as there will be reactions. Furthermore, if one assumes a resolution of 25%, the peak corresponding to 14 MeV neutrons will only be 1/120th the height of the peak due to the recoiling nuclei. It is quite probable that the peak at channel 40 in the last figure is due to these recoiling Li^6 nuclei, while the γ-rays mask the peak which should occur at channel 98.

The next attempt at finding a suitable spectrometer was to use a $Li^6I(Eu)$ crystal in a manner first described by R. B. Murray[4]. It was purchased from the Harshaw Co., mounted in a special bellows with a 1 inch diam. quartz light pipe attached to the 1 inch diam. by

2 mm thick crystal (Fig. 9). This unit was then mounted in a styrofoam and aluminum dewar so that the crystal could be kept at liquid air temperatures. A small chamber held liquid air against the copper on which the crystal was mounted, and this chamber was fed from a reservoir which was kept 3/4 full by means of a float operated valve.

The other end of the quartz light pipe was mounted onto an RCA 6342A photo-multiplier with Dow Corning silicone oil having a viscosity of 3×10^4 centistokes. The $\frac{1}{2}$ inch long end of the light-pipe which protruded beyond the end of the bellows was covered with aluminum foil to reflect light into the photo-multiplier.

The dewar was hollowed out so that a minimum of 1 cm of Fused Boric acid could surround the crystal. This was done in order to cut down the number of epithermal neutrons reaching the crystal, since the latter has a much higher cross-section for these type of neutrons compared with fast neutrons. Cadmium shielding had been tried, but it was found that the resulting γ-rays caused pile up of the pulses, reducing the resolution.

In preliminary runs with this unit, a light pipe extension was made, which resembled a cone, and which matched the 1 inch diam. light pipe to the entire $2\frac{1}{2}$ inch face of the photo-multiplier. This light pipe was made from ultra-violet transmitting lucite, coated with MgO paint. It was found that this light pipe reduced the resolution compared to mounting it directly on the photo-multiplier.

The photo-multiplier was mounted on a pre-amplifier, and compression on the light-pipe-to-p. m. joint was maintained by a pair of springs which ran parallel to the photo-multiplier axis, from the pre-amplifier to the styrofoam dewar.

Fig. 9.

Experimental arrangement of $Li^{6}I(Eu)$ crystal for cooling to Liquid Air temperature.

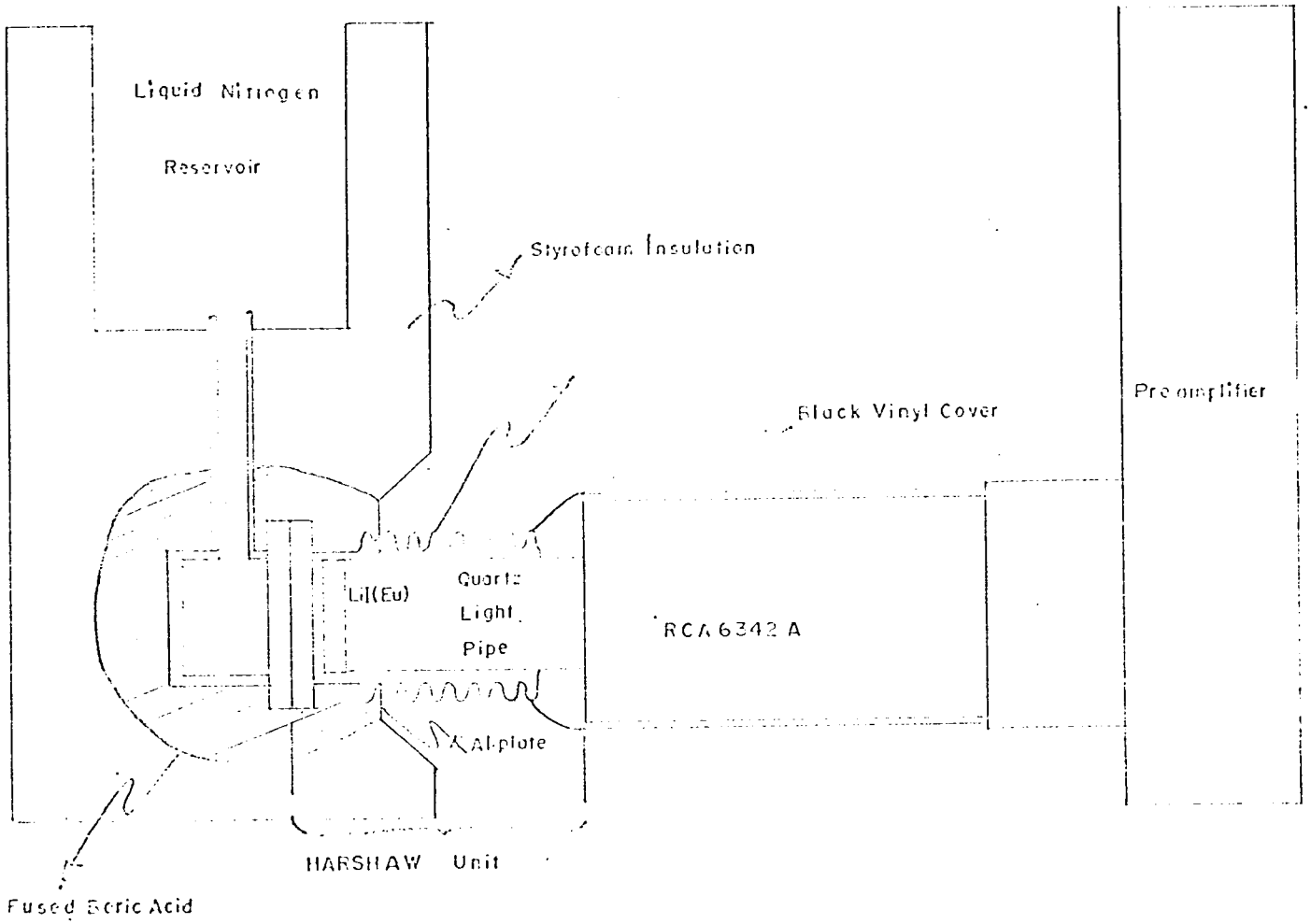
Liquid Nitrogen
Reservoir
Styrofoam Insulation
Black Vinyl Cover
Preamplifier
Li(Eu)
Quartz
Light
Pipe
RCA 6342 A
Al-plate
HARSHAW Unit
Fused Boric Acid

Fig. 10.

Spectra from $Li^{6}I(Eu)$, at temperature of Liquid Air, from 14 MeV neutrons.

a) Original electronics,

b) Selected photo-multiplier and pre-amplifier.

c) With concrete blocks nearby.

(a)

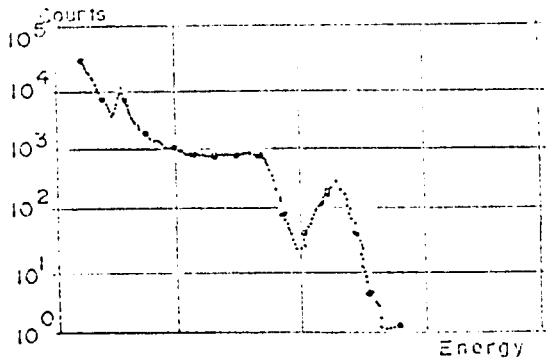
Counts
10^5
10^4
10^3
10^2
10^1
10^0
Energy

(b)

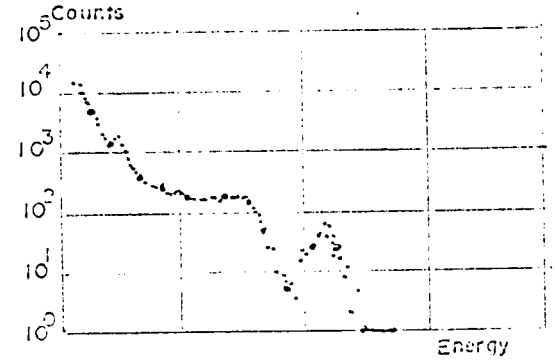
Counts
10^5
10^4
10^3
10^2
10^1
10^0
Energy

(c)

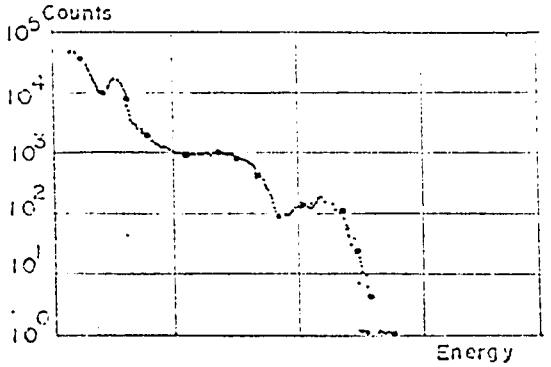
Counts
10^5
10^4
10^3
10^2
10^1
10^0
Energy

A fan was used to blow air across the bellows in an attempt to keep it near room temperature. It was found that the photo-multiplier worked unsatisfactorily when the photocathode went below the freezing point of water.

A word of caution must be given here. Fused Boric Acid is quite exothermic when in contact with water, and it is probable that the crystal could be damaged if condensation water were allowed to get into the shielding material. For this reason, Boron Carbide grinding compound (which has roughly the same shielding efficiency) would be a safer choice.

Fig. 10(a) shows a sample spectrum from the set-up as described above with the pre-amplifier driving a 200 channel kick-sorter. The crystal was irradiated with 14 MeV neutrons resulting in a resolution of 11% corresponding to full width at half max. divided by the channel number. The peak on the upper left hand side corresponds to thermal neutrons, as was verified by placing the system in a large paraffin block with a Ra-Be source. Murray[2] reports a resolution of 5.6%, with a spectrum of simillar general features. He attributes the "shoulder" appearing about midway between the two peaks to competing reactions of the Li^6 with the incoming neutrons.

It was felt that the difficulty in obtaining the resolution found by Murray (5.6%) could have been due to the electronics. In order to check this, the photo-multiplier used in this experiment, and a similar one were attached to 1 3/4 in. dia. by 1 3/4 in. NaI(Tl) crystals, and compared to a Harshaw Integrated 3 in. diam. by 3 in. unit using γ -rays from Cs^{137} and Na^{22}. Three different pre-amplifiers were also used and all combinations of the above were tried. The best photo-multilpier-pre-amplifier combination was then

attached to the $Li^6I(Eu)$ system, and a resolution of 10% for 14 MeV neutrons was obtained. (Fig. 10(b)).

During preliminary experiments with the crystal, it was noted that a peak corresponding to about 2 MeV of γ-ray energy was found when the unit was irradiated with neutrons. Subtraction of the background with a similarly sized crystal of $Li^7I(Eu)$ which is insensitive to neutrons, but has the same behaviour towards γ-rays as the original crystal, failed to remove this peak.

The $Li^6I(Eu)$ unit was then activated under a fairly high flux for 2 minutes, and its γ-ray spectrum recorded with a 3 in. diam. by 3 in. Harshaw Integrated NaI(Tl) crystal. A large peak corresponding to about 1.77 MeV, with a half life of about 2 minutes was seen. It was concluded that this was due to Si in the quartz light pipe, which has a γ-ray of 1.78 MeV and a half life of 2.3 minutes.

It is felt that this would cause serious pile-up problems in fluxes which exceed about 10^6 neutrons per second. A private communication with the Harshaw Company indicated that they had found the same problem, and placed the same upper limit on the flux in which the unit would work.

There is a possibility that neutrons being scattered back from the shielding walls of the laboratory could be causing some of the resolution problems. The walls were made of concrete, whose major constituent by weight (well over 50%) is oxygen. The detector was quite close to the neutron source, and so most of the neutrons returning from the walls would have been scattered through

about 180°. The energy of a neutron, of incident energy Eo, which has been scattered through 180° can be shown to be $E = Eo \frac{(M-m)^2}{(M+m)^2}$ where M is the mass of the scattering nucleus and m the mass of the neutron[5]. The scattering cross-section of oxygen is about equal to those of the other constituents of concrete (1.5 → 2.0 barns), and so the majority of neutrons which enter the detector by way of the shielding walls will have an energy of about 11 MeV. This corresponds to the middle line on the energy scale of the diagrams (Fig. 10).

A run was done using 14 MeV neutrons, and placing several concrete blocks about the counter, in such a way that most of the scattered neutrons hitting the detector would be scattered through 180°. Fig. 10(c) shows the spectrum obtained.

Originally, the dewar had been made from copper and styrofoam, but the copper was a strong source of γ-rays when irradiated with neutrons. An aluminum system was built, which overcame this difficulty, but it cracked one day during pre-cooling, dumping a considerable amount of liquid air on the still warm crystal, causing it to split in two.

It was returned to the Harshaw Company for replacement, and they in turn informed the author that two manufacturing defects had been found which would seriously affect the resolution of the unit. The first was a small vacuum leak in the bellows which caused the crystal to partially dissolve, since it is extremely hygroscopic, and the second was a bare spot in the MgO reflecting paint, which occupied about 10% of the area of the back face of the crystal.

The manufacture of these units requires at least six weeks, and a replacement was not available in time to continue this work.

Conclusions:

Both the "Texlium" and Li^6 loaded glass detectors are unsuitable for the proposed experiment since the energy of the neutrons used would be too high to be detected properly. However, they could be used quite efficiently as spectrometers for neutrons in the range from zero to about 1 MeV.

A properly constructed large BF^3 counter might work, but its large size and low efficiency would make accurate results nearly impossible.

The greatest promise shown so far (aside from very expensive semi-conductor detectors) is from the $Li^6I(Eu)$ crystals. The obvious way to check for interference from neutrons scattered from the walls would be to use a time-of-flight technique like that used on the Li^6 loaded glass. Murray reports a resolution for 14 MeV neutrons of a similar sized crystal of 5.6%.

Because of the time required to overcome the technical difficulties encountered, the program of experiments for examining the spectra from various shielding compounds could not be attempted. However, it is felt that with the resolution achieved by Murray, such a program could be completed.

The dynamitron accelerator anticipated by the physics department should be capable of generating monoenergetic neutrons in the ranges from 0 to 6 MeV and from 11 to 20 MeV. A series of calibration runs at small energy intervals could be done, and the data from these added up on a computor to get the response of the $Li^6I(Eu)$ crystal to a "white" spectrum of neutrons. The energy gap

from 6 to 11 MeV might be filled in by scattering neutrons from a block of paraffin, and selecting energy increments with a time-of-flight system.

An experiment consisting of measuring the spectrum obtained by the crystal from neutrons which traverse a wall of shielding material could be done. At the same time, a high resolution detector of thermal neutrons, such as the texlium detector, could measure the number of such neutrons which are incident on the $Li^6I(Eu)$ crystal.

The spectrum obtained from the crystal could then be subtracted from the measured spectra for a "white" energy distribution previously obtained, and the difference noted. Normalization is possible because of the known number of thermal neutrons. From the "difference spectrum" obtained this way, it would not be difficult to infer what the actual energy spectrum of the emerging neutrons would be.

APPENDIX A

The elastic data has been fitted with the aid of a search program which optimized the parameters of an optical model potential to get the best agreement with the observed scattering cross section. This fit, as well as the Hauser Feshbach and one of the DWB calculations described below, were computed by Dr. D. McPherson of Chalk River Nuclear Laboratories, Chalk River, Ontario, Canada. The potential used was of the form

$$V_{OM} = Vf(r) + iW_g\, g(r) + V_s\, \vec{l}\cdot\vec{s}(\hbar/m_\pi c)^2\, h(r), \qquad (1)$$

where $f(r) = (1 + \exp\ (r - R)/a\ )^{-1}$,

$g(r) = \exp\ -(r - R)^2/b^2$,

$h(r) = \frac{1}{r}\ \frac{d}{dr}\ f(r)$,

and $R = R_o A^{1/3}$.

The smooth curve marked OM on Fig. 6 illustrates the fit which was obtained. The corresponding optical model parameters are given in Table 1. Considering the low mass of the O^{16} nucleus, the agreement between the observed scattering cross section and the optical model result is good. Also, the parameters of Table 1 agree reasonably well with those found by fitting data for 14 MeV neutron scattering on heavier nuclei[5,6,7] with the exception of the spin orbit parameter V_s, which is difficult to determine accurately without measuring the polarization of the scattered neutrons. From the optical model parameters of Table 1,

the integrated elastic and non-elastic scattering cross sections have been calculated. The result for the elastic scattering cross section was 0.87 b which is the same as the experimental value mentioned previously. For the non-elastic cross section the result was 0.61 b which is about 20% lower than the observed value.

A distorted wave Born (DWB) prediction for the direct inelastic scattering excitation of an assumed octupole state at 6.13 MeV in O^{16} has been calculated by Dr. D. McPherson using the optical parameters of Table 2 to define both incoming and outgoing neutron wave functions. No spin-orbit term was included in the interaction. The collective transition was introduced by causing the real part of the potential to undergo an octupole deformation with the magnitude of the DWB cross section being adjusted to fit experiment by varing the collective octupole parameter, β_3. The result is shown on Fig. 6 as a dashed curve marked DWB (real), and the corresponding value of β_3 is 0.68. While this value of β_3 is in reasonable agreement with the value found using proton scattering and with the electromagnetic value, β_3(EM) deduced from a lifetime measurement (see Table 2), the experimental data of Fig. 3 is not well fitted by the DWB cross section. Modifying the optical potential defining the outgoing neutron wave function to account for the energy dependence of the optical model potential did not improve the agreement. Nor did the inclusion of a spin orbit interaction in a similar calculation performed by Dr. G. R. Satchler of the Oak Ridge National Laboratory, Oak Ridge, Tennessee, U.S.A. have much effect on the result. However a DWB calculation, also computed by Dr. Satchler, in which both the real and imaginary parts of the potential were deformed curving the scattering,

does give a slightly better fit [see the smooth curve on Fig. 6 marked DWB (complex)] .

The DWB predictions neglect compound nucleus contributions to the scattering. In order to determine how important this process might be in the case of the 6.13 MeV state, a Hauser-Feshbach statistical calculation has been used to divide up the flux which is absorbed by the imaginary part of the optical potential into all the possible exit channels[4]. In this calculation, the contribution to each channel is weighted according to the optical model transmission coefficient corresponding to that channel. Level densities were required for the nuclides O^{16}, N^{16}, N^{15} and C^{13} which are produced through neutron induced reactions in O^{16}. These were obtained by using known levels and adding a sufficient number of fictitious levels to match the observed level densities for these nuclei[8]. The total inelastic scattering cross section for excitation of all the states in O^{16} by 14.1 MeV neutrons was estimated in this way to be 257 mb. This is close to the sum of the (n, n') cross sections observed in the present work for the 6.1, 7 and 8.9 MeV states plus a probable contribution of about 80 mb for excitation of higher states. (The latter quantity was obtained using (p, p') scattering data for protons having an incident energy near 14 MeV[9]. However the Hauser-Feshbach estimate is based on the assumption that all the inelastic scattering reactions proceed through the compound nucleus stage whereas, in fact, a large portion of the scattering is direct. Thus the estimated cross sections are probably high by a factor of 2 or 3 and should be taken as an upper limit for compound nucleus excitation.

The calculated compound nucleus cross section for excitation of the 6.13 MeV 3- state in O^{16} has been plotted in Fig. 6

(dash-dot curve marked HF). If this cross section is added to either of the DWB results after suitable renormalization of one or both calculated cross sections, the agreement with experiment is worse than for the DWB results done. It is possible that interference between the direct and compound nucleus process is responsible for the poor fit since the estimated compound nucleus contribution is large enough to produce quite sizeable interference terms in the scattering amplitude.

As a matter of interest, the Blair black nucleus diffraction model prediction for direct excitation of an octupole vibration at 6.13 MeV has been included in Fig. 6. This prediction gives a good fit to the data at forward angles and a reasonable value of β_3 (Table 2) despite the assumptions of a sharp edge and total absorption inside the nucleus. The same situation has been found in the case of 14.1 MeV neutron scattering on Ca^{40} and 14.65 MeV proton scattering on several medium weight nuclei[10].

Table 1

Optical model parameters for 14.1 MeV neutrons incident on O^{16}.

R_o (fm)	a (fm)	b (fm)	V (MeV)	W_g (MeV)	V_s (MeV)
1.25	0.52	1.0	-47.2	-5.7	-3.0

Table 2

Values of the collective deformation parameter, β_3, for the 6.13 MeV state in O^{16}.

Experiment	Calculation	R(fm)	β_3	Ref.
Neutron scattering	DWB (real)	3.15	0.68	present work
	DWB (complex)	3.15	0.64	present work
	Blair	5.7	0.47	
Proton scattering	DWB (real)		0.59	3)
	DWB (complex)		0.48	3)
Electromagnetic lifetime measurement[a]			+0.40 -.72-0.20	18)
Single Particle	$\beta_3 = 1.563/Z$		0.20	3)

a) Deduced from the lifetime by assuming a charge distribution in agreement with that found from electron scattering measurements, namely $R_o = 1.1$ fm and $a = 0.55$ fm where the form of the distribution is given by f(r) of equation 1.

Conclusions.

The $O^{16}(n,n')O^{16}$ reaction has been studied in some detail using data from both neutron and gamma ray measurements. Differential scattering cross sections were obtained for neutrons scattered from states in O^{16} at 0, 6.1, 7 and 8.9 MeV. In addition there was evidence for excitation of a state near 11 MeV although an angular distribution of the scattered neutrons was not obtained. The strongest excitation occurred at 6.1 MeV. A comparison of the 6.1 MeV excitation cross section obtained from the neutron measurement with that deduced from the gamma ray work indicates that the O^{16} level responsible was the 3-state at 6.13 MeV and not the 0+ state at 6.05 MeV.

A good fit has been obtained for the elastic scattering data using an optical model with reasonable well parameters. However, attempts to fit the observed cross section for excitation of the 6.13 MeV 3-state using DWB predictions for direct excitation of a collective octupole vibration were not very successful. It is likely that the difficulty lies in the use of the DWB treatment rather than the assumption of an octupole nature for the excited state because the shapes of DWB angular distributions are generally insensitive to internal nuclear wave functions. The values of β_3 needed to normalize the DWB results imply a strong collective enhancement for the 3-state. Thus a coupled equation calculation might give a better result than the simple DWB treatment. Somewhat surprisingly, the Blair model, which assumes a sharp edged black nucleus, yielded a fairly good fit to the angular distribution at forward angles and in addition gave a reasonable value for β_3.

APPENDIX B

The Born Approximation:

The Born approximation consists in saying that the scattered wave in a nuclear scattering process is small compared to the incident wave, and that every point of the scattering potential sees the same incident amplitude. This approximation obviously works only for those cases where the scattering cross-section is small.

This allows the resulting Schroedinger Equation to be solved in terms of a Greens function which gives a scattering amplitude (or corss-section, since they are related) in terms of the change in wave number, the scattering potential, and a position vector within the scattering potential[11]. At high incident energies (> 10 MeV) a monoenergetic beam of particles could be represented as a series of plane waves incident on solid sphere. This resulting Plane Wave Born Approx. assumes that the scattering potential does not affect the incoming waves other than changing their direction within the scattering potential.

When conservation of the angular momentum between the incident and scattered systems is demanded, a scattering amplitude, which is a function of the scattering angle, results, and this gives rise to an angular distribution of the scattered particles.

The Distorted Wave Born Approx. takes into account the fact that the incident wave is distorted by the scattering potential. The scattered wave is represented by an outgoing spherical wave and the interaction of the two different waves produces a distorted plane

wave, which is allowed to interact with a standard optical model potential.

In the case of inelastic scattering, the wave number and the optical model potential both change. This is mathematically approximated by considering an incident beam having the new momentum incident on an optical model potential corresponding to the excited state of the nucleus. By invoking time reversal, this calculation is used for the matrix element corresponding to the scattered wave, in the expression for the scattering amplitude.

Collective excitations of the nucleus can sometimes be studied with DWBA. A "search program" is used to find the best optical model parameters which fit the problem being studied. A dipole, quadrupole, octupole ... (depending upon the state under study), deformation is then imposed on the real part or the real and imaginary parts of the optical model potential, and an improvement in the fit between experimental data and theoretical predictions is sought[6].

The Blair Model.

The Blair Model makes use of the fact that many of the heavier nuclei appear as if the absorption takes place within a volume given by a fairly well defined radius. For relatively small angle scattering, this nucleus can be approximated by a black disc, and all the scattering reactions take place in the surface region (corresponding to the edge of the disc.). The mathematics of Fraunhoffer diffraction theory can be applied to this problem and the angular distribution (after insisting on conservation of angular momentum) arises in a scattering amplitude term which contains Bessel's functions.

If collective deformations of the nucleus are considered, (in terms of spherical harmonic functions) and the scattering process is "adiabatic" (i. e., the scattering event takes place in a time which is short compared with collective motions of the nucleus), then secondary terms involving Bessel's functions appear, which correspond to distortions of the normal Fraunhoffer diffraction pattern from a circular object. By comparing these distortions in the angular distribution with experimental differential scattering cross-sections, inference can be made as to the shape of the scattering nucleus and its excited states[12].

A. Dar shows that the Blair model assumes that the inelastic scattering reaction takes place on the edge of a "Black Disc".[13] He points out that in actual fact, an entire region corresponding to a layer around the outside of this black nucleus gives rise to these reactions. He modifies Blairs calculations by assuming that the black disc is really an annulus of a fixed width from which coherrent waves emanate and give rise to interference effects.

The result of this is an exponentially decaying function of scattering angle added to which is a set of terms which involve Bessel's functions. These arise in the same sort of way as in Blair's calculations (by considering deformations of the nuclei) but the relative variations in scattering amplitude with angle are smoothed out, and are in much better agreement with experiment.

In all of these theories, if the nucleus has a collective deformation, it can be described in terms of a sum of spherical harmonics multiplied by a coefficient which indicates the contribution of each harmonic. If the nucleus has a permanent ground state deformation, then all the coefficients in the sum describing this

deformation can be combined into a "Collective deformation parameter ". In the case of collectively deformed excited states, an effective (root mean square) deformation parameter, β , is defined in a similar manner.

The diffraction pattern created by an object will be affected by the shape of that object (eg. circular, elliptical, etc.) and one would expect that the deformation parameter β_λ would show up in the expressions for the angular distribution of the scattered particles. With a suitable optical potential, one can vary β_λ in order to get the best fit in the above theories, and thus get some idea of the type and amount of distortion of the nucleus.

Compound Nucleus.

There is a probability, especially at low incident energies, that the incoming neutron will be "captured" by the target nucleus[3]. This is represented in the Optical Model by an imaginary part of the potential. The incoming particle can interact with one or more low level, or ground state nucleons in the target, and lose so much energy in the process that it cannot escape the nuclear potential. The nucleus must then wait until some nucleon, by chance, gets enough energy to escape and carry off this excess energy. Such a process requires about 10^{-16} seconds compared with the 10^{-21} seconds required for a direct interaction.

The term "level density" refers to the number of available energy levels per energy increment for a given nucleus. If the level density of a target nucleus is high, or the energy of the incident particle is high, then the nucleons which are ejected from the

compound nucleus appear to boil-off, since their energy distribution is Maxwellian, and the angular distribution is isotropic.

The Hauser-Feshbach theory[4] demonstrates that this should be so, and shows also that if the level density is low, or the incident energy only moderate, that the total cross-section, as well as the energy and angular distribution of the emergent particles is sensitive to the energy, angular momentum and parity differences which exist between the ground state of the target nucleus, and the states excited.

APPENDIX C

Optimum Time of Flight Arrangement

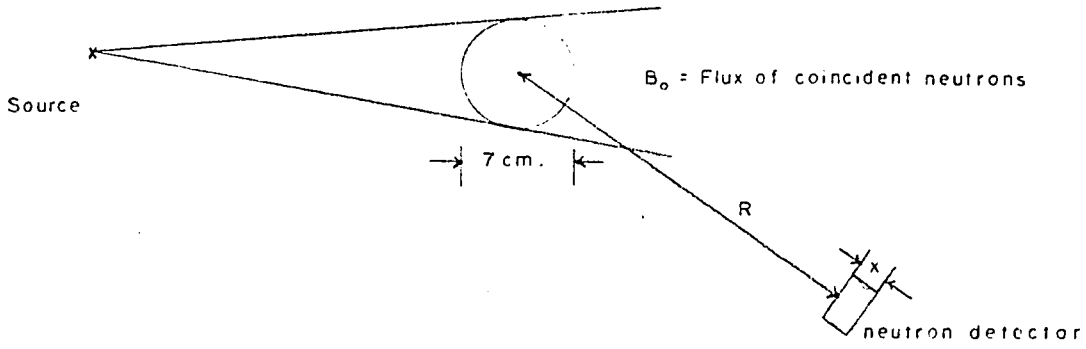

Conditions: B_o is a constant set by the pile-up of pulses in the associated particle detector. The electronics is stable for 48 hours and about 3000 counts are required in the neutron detector for good statistics. This gives a rate of 3×10^{-2} counts per second.

Problem: What values of R and X will give the best time resolution?

The number of neutrons scattered from the target, out of the coincidence beam, is $B = B_o(1-e^{-N\sigma y})$

where $N = \frac{\text{No. of atoms}}{\text{cm}^3}$

σ = cross-section

and y = 7 cm.

$N = 6 \times 10^{23} \times 1.15 \div 16 = .43 \times 10^{23} = 4.3 \times 10^{22}$

σ for $O^{16} \approx 1.5$ b $= 1.5 \times 10^{-24}$ cm^2

$$\therefore \quad N\sigma y = 4.3 \times 10^{22} \times 1.5 \times 10^{-24} \times 7 = 45 \times 10^{-2}$$

$$e^{-.45} = .64 \text{ and } 1 - .64 = .36$$

$$\therefore \quad B = .36\, B_o \text{ in all directions} \tag{1}$$

The number of neutrons incident per sec. on the neutron detector of area A is

$$\frac{BA}{4\pi R^2} = \frac{.36 B_o A}{4\pi R^2} = F_o(R) \tag{2}$$

A 5 cm thick detector had an efficiency of .136, i.e.

$$N_1 \tilde{\sigma}_o X_1 = .136$$

where N_1 is the number of atoms/cm^3 and $\tilde{\sigma}_o$ their cross-section

$$\therefore \quad N_1 \tilde{\sigma}_o = \frac{.136}{5} = 2.7 \times 10^{-2}\ cm^{-1}$$

The number of neutrons detected per second = $F(R) = F_o(R)(1-e^{-N_1 \tilde{\sigma}_o X})$

$$\text{i.e.} \qquad F(R) = F_o(R)(1-e^{-.027X}) \tag{3}$$

The time resolution of the system = $\Delta T / \frac{R}{V}$ where V is $\frac{1m}{20\ n\ sec}$ (the velocity of a 14 MeV neutron) and ΔT is the time jitter arising from the finite size of the target and detector.

$$\text{i.e.} \quad \Delta T = \sqrt{(\Delta T \text{ target})^2 + (\Delta T \text{ det})^2}$$

Assuming a target thickness of 7 cm = .07m, ΔT targ. = $.07 \times 20 \times 10^{-9}$ sec. and $(\Delta T \text{ targ})^2 \approx 2 \times 10^{-18}$ sec^2 and $(\Delta T \text{ det})^2 = (400 \times 10^{-18} \times X^2 \times 10^{-4})$ sec^2

$$\therefore \Delta T = \left\{2 \times 10^{-18} + .04X^2 \times 10^{-18}\right\}^{\frac{1}{2}} = 10^{-9}\sqrt{2 + .04X^2} \text{ sec.}$$

Thus the time resolution M that must be kept to a minimum is

$$M = \frac{\sqrt{2 + .04X^2}}{20R} \tag{4}$$

where X is in cm and R is in metres.

The following conditions apply to M:

$$F(R) = F_o(R)\,(1-e^{-.027X}) \geq 2 \times 10^{-2} \text{ sec}^{-1} \tag{3}$$

where $$F_o R = .36\, B_o A/4\pi R^2 \tag{2}$$

The Area A of the detector is $.031 \text{ m}^2$

$$\therefore \quad F(R) = 11.2 \times 10^{-3} \times \frac{B_o}{R^2}\,(1-e^{-.027X})$$

Choosing the equality condition in equation (3) one gets

$$2 \times 10^{-2} = 11.2 \times 10^{-3}\ \frac{B_o}{R^2}\ (1-e^{-.027X})$$

$$\text{or} \qquad R^2 = 5.6 \times 10^{-1} B_o\,(1-e^{-.027X}) \tag{5}$$

Now consider M. If it is to have meaning, it must be positive and greater than zero. The values of X and R for which M is a minimum

are the same as for when M^2 is a minimum. Thus substituting (5) into (4) and squaring:

$$M^2 = \frac{2 + .04X^2}{.56B_o(1-e^{-.027X})(400)}$$

$$\frac{d(M^2)}{dx} = \frac{(224B_o(1-e^{-.027X})(.08X) - (2 + .04X^2)(224B_o \times .027e^{-.027X})}{224B_o(1-e^{-.027X})^2} = 0 \text{ for min.}$$

$$\therefore \quad (224B_o)(.08X)(1-e^{-.027X}) = 2(224B_o)(.027e^{-.027X}) +$$

$$+ (.04X^2)(224B_o)(.027e^{-.027X})$$

Divide by $224B_o$,

$$\ldots \quad (1-e^{-.027X})(.08X) - (2 + .04X^2)(.027e^{-.027X}) = 0$$

or

$$e^{-.027X}(.08X + .054 + 10.8 \times 10^{-4} X^2) - .08X = 0$$

This equation was worked out numerically for values of X lying between .5 and 100 and a solution was found at X = 6.7 cm. Putting this value for the thickness of the detector into equation (5), one gets

$$R^2 = .56B_o(1-e^{-.027X}) = .56B_o(1-.835)$$

$$= .56B_o(.165) = .0923B_o$$

In the arrangement used for the O^{16} experiment, the best flux obtainable was $B_o = 3.3 \times 10^2$ sec^{-1}, otherwise pile up in the detector would occur.

$$\therefore \quad R^2 = .0923 \times 3.3 \times 10^2 = 3.02 \text{ m}^2$$

$$\text{and } R = 1.74 \text{ metres.}$$

The slab used had a thickness of 5 cm. Here, $R^2 = 3.3 \times 10^2 \times .874 \times .56$ or $R^2 = 1.6 \text{ m}^2$ whence R = 1.3 m.

It should be noted that some of the data, (R = 2.3 m) had less than 10^3 counts in 48 hours, and was difficult to analyse.

APPENDIX D

ANALYSIS OF TEXLIUM DETECTOR.

The reaction upon which this detector is based is:

$$He^3 + n \rightarrow H^3 + H^1 + 764 \text{ KeV.}$$

It is of interest to find the range of the triton and proton given off in this reaction, since it is felt that some of the energy which should be lost in the gas is actually going into the walls of the counter.

Consider the case of 2.5 MeV neutrons incident on the detector. The total energy available to the two particles is;

$$E_t = 2.5 + .8 = 3.3 \text{ MeV}$$

In centre of mass coordinates.

$$M_t V_t = M_p V_p$$

where t refers to the triton and p to the proton.

$$\therefore \quad V_t/V_p = M_p/M_t = 1/3 \qquad (1)$$

By conservation of energy, $\frac{1}{2}M_t V_t^2 + \frac{1}{2}M_p V_p^2 = 3.3$ MeV.

or

$$M_t V_t^2 + M_p V_p^2 = 6.6 \text{ MeV.} \qquad (2)$$

$$M_p + M_t \frac{V_t^2}{V_p^2} = \frac{6.6}{V_p^2}$$

or $$M_p + M_t \times (1/3)^2 = \frac{6.6}{V_p^2} \quad \text{from (1)}$$

$$\therefore \quad M_p V_p^2 + \frac{1}{9} M_t V_p^2 = 6.6$$

$$\because \quad M_t V_p^2 = 3 M_p V_p^2, \quad \therefore \quad \frac{4}{3} M_p V_p^2 = 6.6$$

or $$\tfrac{1}{2} M_p V_p^2 = \frac{3}{8} \times 6.6 = 2.5 \text{ MeV}$$

$$\therefore \quad E_p = 2.5 \text{ MeV and } E_t = .8 \text{ MeV}$$

To find the range of a triton in a gas, one needs to know the energy of a proton having the same velocity as the triton (see Evans, "The Atomic Nucleus" p. 650),

$$V_t = \sqrt{1.6/M_t} = V'_p$$

$$E'_p = \tfrac{1}{2} M_p V'^2_p = \tfrac{1}{2} M_p \frac{1.6}{M_t} = \tfrac{1}{2} \cdot \frac{1.6}{3} \quad \left(\because \frac{M_p}{M_t} = \frac{1}{3}\right)$$

$$\therefore \quad E'_p = .27 \text{ MeV}$$

From Evans, $R_t/R_p = 3$ where R is the range

and $R_p(.27 \text{ MeV}) = 1 \text{ cm.} \quad \therefore \quad R_t = 3 \text{ cm. in air.}$

$R_p(2.5 \text{ MeV}) = 10 \text{ cm.}$

The Bragg-Kleeman Equation as applied to gasses can be written as follows:

$$\frac{R_1}{R_o} = \frac{M_o}{M_1} \quad \frac{\sqrt{A_1}}{\sqrt{A_o}}$$

where M is the atomic mass and A the atomic No.

The ranges of two particles may, to a first approximation, be added to get an effective range in air. This is not strictly correct since the reaction is not isotropic as was assumed earlier.

Then the total Range R_1 = 13 cm in air at 1 Atm. and 15°C.

Now the range in 1 Atm of Krypton =

$$\frac{28}{85} \times \frac{6}{3.81} \times 13 \text{ cm} = 7.0 \text{ cm.}$$

The range in 2 Atm of Kr is 3.5 cm.

The range in 1 Atm of He^3 =

$$\frac{28}{3} \times \frac{1.41}{3.81} \times 13 = 45 \text{ cm.}$$

The range in 4 Atm of He^3 is 11 cm.

The range in a mixture of these two gasses is then given by:

$$\frac{1}{R} = \frac{1}{R_{Kr}} + \frac{1}{R_{He^3}}$$

$$= \frac{1}{3.5} + \frac{1}{11} = \frac{11 + 3.5}{38.5} = \frac{14.5}{38.5}$$

$$\therefore \quad R = \frac{38.5}{14.5} = 2.66 \text{ cm.}$$

The diameter of the counter is 2.54 cm.

Let the Range of the two particles in the gas be considered as 2.54 cm (an error of 5% which offsets the previous errors made in adding the two individual ranges). The problem then remains to find what proportion of all the events which take place in the counter gas will give rise to a pulse corresponding to the full energy of 3.3 MeV.

To do this, consider a cylinder of DiameterD, intersecting a sphere of radius R such that the centre of the sphere always lies within the cylinder (see diagram). What proportion of the total solid angle of the sphere is generated by those portions of the surface area of the sphere lying within the cylinder?

When this problem is set up, R will be set equal to D, and the centre of the sphere will be allowed to range over the entire cross-sectional area of the cylinder.

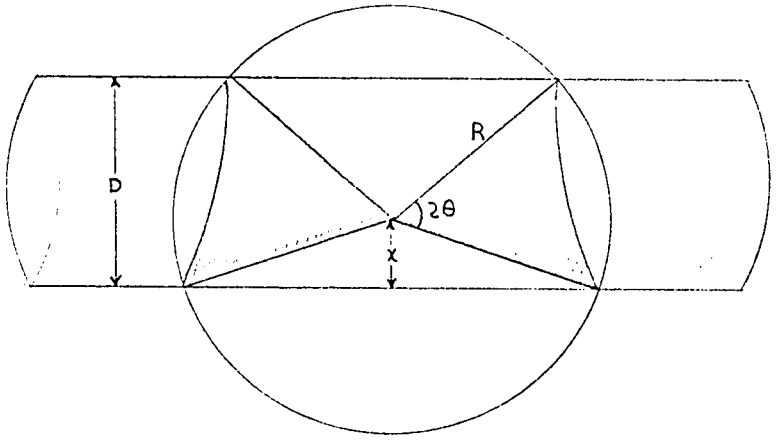

Let Ω be the solid angle corresponding to 2θ. Then the total solid angle is 2Ω.

$$\Omega = 2\pi(1-\cos\theta) \quad \text{and} \quad 2\Omega = 4\pi(1-\cos\theta)$$

The fraction of this compared with the total solid angle of a sphere is

$$P = 1-\cos\theta$$

Now $$2\theta = \pi - \cos^{-1}\frac{x}{R} - \cos^{-1}\frac{D-x}{R}$$

$$\therefore \quad \theta = -\left(\tfrac{1}{2}\cos^{-1}\frac{x}{R} + \tfrac{1}{2}\cos^{-1}\frac{D-x}{R}\right) + \frac{\pi}{2}$$

and $$P = 1 + \cos^{\frac{1}{2}}\left\{ \underbrace{\cos^{-1}\frac{x}{R}}_{M} + \underbrace{\cos^{-1}\frac{D-x}{R}}_{N} \right\} \quad \text{and } \frac{x}{R} = X, \frac{D-x}{R} = Y$$

$$\cos\tfrac{1}{2}(M+N) = \cos\frac{M}{2}\cos\frac{N}{2} - \sin\frac{M}{2}\sin\frac{N}{2}$$

$$= \pm\sqrt{\frac{1+\cos M}{2}}\sqrt{\frac{1+\cos N}{2}} \mp \sqrt{\frac{1-\cos M}{2}}\sqrt{\frac{1-\cos N}{2}}$$

$$= \pm\tfrac{1}{2}\left\{\sqrt{1+X}\sqrt{1+Y} \mp \sqrt{1-X}\sqrt{1-Y}\right\}$$

$$= \pm\tfrac{1}{2}\left\{\sqrt{1+X+Y+XY} \mp \sqrt{1-X-Y+XY}\right\}$$

$$= \pm\tfrac{1}{2}\left\{\sqrt{1+\frac{x}{R}+\frac{D-x}{R}+\frac{xD-x^2}{R^2}} \mp \sqrt{1-\frac{x}{R}-\frac{x+D}{R}+\frac{xD-x^2}{R^2}}\right\}$$

$$= \pm\tfrac{1}{2}\left\{\sqrt{1+\frac{D}{R}+\frac{xD-x^2}{R^2}} \mp \sqrt{1-\frac{2x+D}{R}+\frac{xD-x^2}{R^2}}\right\}$$

$$\text{Now } R = D = \pm\frac{1}{2}\left\{\sqrt{2 + \frac{xR-x^2}{R^2}} \mp \sqrt{\frac{2x}{R} + \frac{xR-x^2}{R^2}}\right\}$$

$$= \pm\frac{1}{2R}\left\{\sqrt{2R^2 + xR-x^2} \mp \sqrt{3xR - x^2}\right\}$$

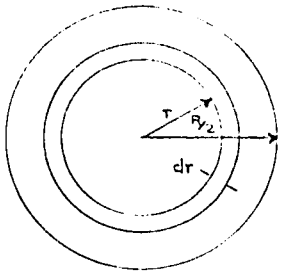

Area of ring $= 2\pi r dr$ Area of circle $= \pi R^2/4$

Now the No. of events in ring is proportional to $\frac{8\pi r dr}{\pi R^2} = \frac{8}{R^2} r dr$

and $x = \frac{R}{2} - r$.

$$2R^2 + xR-x^2 = 2R^2 + \frac{R^2}{2} - Rr - \frac{R^2}{4} + Rr-r^2$$

$$= \frac{5}{2}R^2 - r^2$$

$$\text{and } 3xR-x^2 = \frac{3}{2}R^2 - 3rR - \frac{R^2}{4} + Rr-r^2$$

$$= \frac{5}{4}R^2 - 2rR - r^2$$

$$\int_o^{R/2} r\sqrt{\frac{5}{2}R^2 - r^2}\, dr = -\frac{1}{3}X\sqrt{X}\Big|_o^{R/2}$$

$$\int_o^{R/2} r\sqrt{\frac{5}{4}R^2-2rR-r^2}\, dr = -\frac{1}{3}X\sqrt{X}\Big|_o^{\frac{R}{2}} - R\int_o^{\frac{R}{2}}\sqrt{X}\, dx = -\frac{1}{3}X\sqrt{X}\Big|_o^{\frac{R}{2}} -$$

$$- R\,\frac{(-2r-2R)\sqrt{X}}{-4}\Big|_o^{\frac{R}{2}} + \ldots$$

$$\int_0^{\frac{R}{2}} r\sqrt{\frac{5}{4}R^2 - 2rR - r^2}\,dr = \frac{1}{3}X\sqrt{X}\Big|_0^{\frac{R}{2}} - R\int_0^{\frac{R}{2}}\sqrt{X}\,dx$$

$$= -\frac{1}{3}X\sqrt{X}\Big|_0^{\frac{R}{2}} - R\left(\frac{2r+2R}{4}\sqrt{x}\right)\Big|_0^{\frac{R}{2}} + \frac{R}{2k}\int_0^{\frac{R}{2}}\frac{dr}{\sqrt{X}}$$

Now $k = \frac{-4}{q}$ and $q = -4 \times \frac{5}{4}R^2 - 4R^2 = -9R^2$

$$\therefore k = \frac{4}{9R^2}$$

$$\therefore \int_0^{\frac{R}{2}} r\sqrt{X} = -\frac{1}{3}X\sqrt{X}\Big|_0^{\frac{R}{2}} - R\left(\frac{r+R}{2}\sqrt{X}\right)\Big|_0^{\frac{R}{2}} + \frac{9R^3}{8}\,\mathrm{Sin}^{-1}\,\frac{2r+2R}{\sqrt{4R^2+5R^2}}\Big|_0^{\frac{R}{2}}$$

$$= -\frac{1}{3}X\sqrt{X}\Big|_0^{\frac{R}{2}} - R\left(\frac{r+R}{2}\sqrt{X}\right)\Big|_0^{\frac{R}{2}} + \frac{9R^3}{8}\,\mathrm{Sin}^{-1}\left(\frac{2r+2R}{\sqrt{9R^2}}\right)\Big|_0^{\frac{R}{2}}$$

$$= -\frac{1}{3}X\sqrt{X}\Big|_0^{\frac{R}{2}} - R\left(\frac{r+R}{2}\sqrt{X}\right)\Big|_0^{\frac{R}{2}} + \frac{9}{8}R^3\,\mathrm{Sin}^{-1}\left(\frac{2r+2R}{3R}\right)\Big|_0^{\frac{R}{2}}$$

Now $\sqrt{X}\Big)_{\frac{R}{2}} = r = \sqrt{\frac{5}{4}R^2 - R^2 - \frac{R^2}{4}} = 0$

$$\sqrt{X}\Big)_{r=0} = \sqrt{\frac{5}{4}R^2} = \frac{R}{2}\sqrt{5}$$

$$\therefore \int_0^{\frac{R}{2}} r\sqrt{X} = -\frac{1}{3}X\sqrt{X}\Big|_0^{\frac{R}{2}} - R^2\cdot\tfrac{1}{2}\cdot\frac{R}{2}\sqrt{5} + \frac{9}{8}R^3\underbrace{\left(\mathrm{Sin}^{-1}1 - \mathrm{Sin}^{-1}\frac{2}{3}\right)}_{\frac{\pi}{2}-\frac{\pi}{4}}$$

The total No. of events giving rise to pulses with full energy is:

$$\frac{8}{R^2}\int_0^{\frac{R}{2}} r\,dr\,(1+\cos\tfrac{1}{2}(M+N)$$

$$= \frac{8}{R^2} \int_0^{\frac{R}{2}} r\,dr \; (1 + \cos\tfrac{1}{2}(M + N))$$

$$= \frac{8}{R^2} \cdot \tfrac{1}{2} \cdot \frac{R^2}{4} + \frac{8}{R^2} \int_0^{\frac{R}{2}} r \cos\tfrac{1}{2}(M + N)\, dr$$

$$= 1 + \frac{8}{R^2}\left\{ \begin{matrix} + \\ - \end{matrix} \frac{1}{2R}\left(-\frac{1}{3} X\sqrt{X} \Big|_0^{\frac{R}{2}} \begin{matrix} - \\ + \end{matrix} \left[-\frac{1}{3} X\sqrt{X} \Big|_0^{\frac{R}{2}} - \right.\right.\right.$$

$$\left.\left.\left. - \frac{\sqrt{5}}{4} R^3 + \frac{9}{8} R^3 \frac{\pi}{4} \right]\right)\right\}$$

$$= 1 - \frac{4}{R^3}\left(\frac{\sqrt{5}}{4} R^3 + \frac{9\pi}{32} R^3\right) = 1 - \sqrt{5} + \frac{9\pi}{8} = 1 - 2.25 + 3.5$$

$$= \frac{1}{4}$$

Extraneous Solution: $1 + \sqrt{5} - \frac{9}{8}\pi = 1 + 2.25 - 3.5 = -\frac{1}{4}$

Thus, only one quarter of all the events taking place in the counter will give rise to a peak corresponding to the energy of the incident neutrons plus the Q of the reaction.

PART I

REFERENCES

1) W. John MacDonald. Thesis towards Ph. D. degree "Excited States in Ca and 0_2". 1964. University of Ottawa.

2) G. Glavina. M. Sc. Thesis, University of Ottawa, Canada (unpublished).

3) Problems of Nuclear Structure. V. F. Weisskopf, Phys. Today, July 1961.

4) Hauser and Feshbach. Phys. Rev. 87 (1952) 366.

5) R. L. Clarke and W. G. Cross. Nuclear Physics 53 (1964) 177.

6) W. J. MacDonald and J. M. Robson. Nuclear Phys. 59 (1964) 321.

7) F. E. Bjorklund and S. Fernbach. Phys. Rev. 109 (1968) 1295.

8) F. Ajzenberg-Selove and T. Lauritsen. Landolf-Bornstein, group 1, 1 (1961) 1-54.

9) S. Kobayashi. Jour. Phys. Soc., Japan, 15 (1960) 1164.

10) K. Matsuda. Nuclear Phys. 33 (1962) 536.

11) Dicke and Wittke, Introduction to Quantum Mechanics, section 16-2, Adison-Wesley 1960.

12) J. S. Blair. Phys. Rev. Vol. 115, No. 4, pp. 928.

13) A. Dar. Nucl. Phys. 55 (1964) 305-321.

PART II AND APPENDICES

REFERENCES

1) J. M. Robson and C. Glavina. The Attenuation of fast neutrons by Carbon. (unpublished).

2) Neutron Cross-Sections. Supplement No. 1 to Second Edition 1960.

3) Firk, Slaughter and Ginther. Nucl. Inst. 13 (1961) p. 314.

4) R. B. Murray. Use of Li^6(Eu) as a Scintillation Detector and Spectrometer for Fast Neutrons. Nucl. Instr. 2 (1958) 237-248.

5) I. Kaplan. Nuclear Physics. Adison-Wesley, 1955.